Toxicology and Applied Pharmacology 482 (2024) 116784

Contents lists available at ScienceDirect

Toxicology and Applied Pharmacology

journal homepage: www.elsevier.com/locate/taap

Mechanisms related to carbon nanotubes genotoxicity in human cell lines of respiratory origin

Liliya M. Fatkhutdinova [a,*], Gulnaz F. Gabidinova [a], Amina G. Daminova [b], Ayrat M. Dimiev [c], Timur L. Khamidullin [c], Elena V. Valeeva [a], Agboigba Esperant Elvis Cokou [b], Shamil Z. Validov [b], Gyuzel A. Timerbulatova [a]

[a] Kazan State Medical University, Kazan 420012, Russian Federation
[b] Kazan Federal University, Kazan 420008, Russian Federation
[c] Kazan Federal University, Laboratory for Advanced Carbon Nanomaterials, Kazan 420008, Russian Federation

ARTICLE INFO

Editor: Lawrence Lash

Keywords:
Carbon nanotubes
Human cell lines of respiratory origin
DNA comet assay
Nuclear translocation
Oxidative stress
Transmission electron microscopy

ABSTRACT

Potential genotoxicity and carcinogenicity of carbon nanotubes (CNT), as well as the underlying mechanisms, remains a pressing topic. The study aimed to evaluate and compare the genotoxic effect and mechanisms of DNA damage under exposure to different types of CNT.

Immortalized human cell lines of respiratory origin BEAS-2B, A549, MRC5-SV40 were exposed to three types of CNT: MWCNT Taunit-M, pristine and purified SWCNT TUBALL™ at concentrations in the range of 0.0006–200 μg/ml. Data on the CNT content in the workplace air were used to calculate the lower concentration limit. The genotoxic potential of CNTs was investigated at non-cytotoxic concentrations using a DNA comet assay. We explored reactive oxygen species (ROS) formation, direct genetic material damage, and expression of a profibrotic factor *TGFB1* as mechanisms related to genotoxicity upon CNT exposure.

An increase in the number of unstable DNA regions was observed at a subtoxic concentration of CNT (20 μg/ml), with no genotoxic effects at concentrations corresponding to industrial exposures being found.

While the three test articles of CNTs exhibited comparable genotoxic potential, their mechanisms appeared to differ. MWCNTs were found to penetrate the nucleus of respiratory cells, potentially interacting directly with genetic material, as well as to enhance ROS production and *TGFB1* gene expression. For A549 and MRC5-SV40, genotoxicity depended mainly on MWCNT concentration, while for BEAS-2B – on ROS production. Mechanisms of SWCNT genotoxicity were not so obvious. Oxidative stress and increased expression of profibrotic factors could not fully explain DNA damage under SWCNT exposure, and other mechanisms might be involved.

1. Introduction

The incorporation of novel nanomaterials into industrial practices necessitates a comprehensive understanding of their implications for both human health and the environment. Carbon nanotubes (CNT) possess unique physicochemical properties that have led to their expanded production and application. CNTs improve the mechanical, electrical, and thermal properties of composite materials (Eatemadi et al., 2014; Nurazzi et al., 2021a). The distinct properties exhibited by CNTs have opened up extensive opportunities for their integration into the fields of construction (Eatemadi et al., 2014; Nurazzi et al., 2021a), nanoelectronics (Ajori et al., 2015; Zhou et al., 2018; Nurazzi et al., 2021a), nanobiotechnology (Chen et al., 2003; Cherukuri et al., 2004; Liu et al., 2009). CNTs are used in composites to enhance corrosion protection (Hassan et al., 2020; Souto and Soares, 2020), applied in solar cell technologies (Chen et al., 2017; Chen et al., 2019a; Chen et al., 2018; Chen et al., 2020), chemical sensors (Janudin et al., 2018; Maity et al., 2018; Nurazzi et al., 2021b), and storage batteries (Chen et al., 2019b; Guo et al., 2019). Given the increasing commercial potential of CNTs, it becomes imperative to conduct safety research on this type of nanomaterials.

Potential genotoxicity of nanomaterials, including carbon nanotubes, is among the primary concerns. Experiments conducted on laboratory animals have demonstrated the carcinogenic properties of multi-

* Corresponding author: Department of Hygiene and Occupational Medicine, Kazan State Medical University, 49, Butlerova Street, Kazan 420012, Russian Federation.
E-mail address: liliya.fatkhutdinova@kazangmu.ru (L.M. Fatkhutdinova).

https://doi.org/10.1016/j.taap.2023.116784
Received 11 October 2023; Received in revised form 28 November 2023; Accepted 2 December 2023
Available online 7 December 2023

walled carbon nanotubes (MWCNT) MWCNT-7 (Mitsui Ltd., Japan) and MWCNT-N (NIKKISO, Japan), leading to the formation of mesothelioma, bronchiolo-alveolar adenoma, and adenocarcinoma (Chernova et al., 2017; Hojo et al., 2022; Nagai et al., 2013; Sakamoto et al., 2009; Sargent et al., 2014; Snyder-Talkington et al., 2016; Suzui et al., 2016; Takagi et al., 2008; Takagi et al., 2012). MWCNT-7 (Mitsui Ltd., Japan) have been classified as a possible human carcinogen (group 2B) by the International Agency for Research on Cancer (IARC) (Grosse et al., 2014). However, the carcinogenicity of single-walled carbon nanotubes (SWCNT) in experiments *in vivo* was not proven. Meanwhile, potential pulmonary toxicity is associated with SWCNTs, which manifests in acute and chronic inflammation, granuloma formation, collagen deposition, and fibrosis development (Ema et al., 2017; Erdely et al., 2013; Mutlu et al., 2010; Poland et al., 2008; Shvedova et al., 2005; Shvedova et al., 2007; Shvedova et al., 2008; Shvedova et al., 2013; Shvedova et al., 2014; Teeguarden et al., 2011; Wang et al., 2010; Wang et al., 2016), has been reported.

The investigation of the genotoxic and carcinogenic capabilities of CNTs, as well as the underlying mechanisms, remains a pressing topic. The inhalation route of entry identifies the respiratory system as the most likely target of the toxic effects of industrial CNTs. Several *in vivo* and *in vitro* studies have demonstrated the genotoxic potential of MWCNTs and SWCNTs in relation to the respiratory system (Di Ianni et al., 2021; Lan et al., 2014; Lindberg et al., 2013; Poulsen et al., 2016; Solorio-Rodriguez et al., 2023; Wils et al., 2021a], while opposite results were obtained in other experiments (Honda et al., 2017; Knudsen et al., 2019; Louro et al., 2016; Pothmann et al., 2015; Rahman et al., 2017; Solorio-Rodriguez et al., 2023; Vales et al., 2016). Discrepancies in experimental data might indicate that a risk assessment should be carried out for each type of CNTs.

The direct genotoxicity mechanism of CNTs can manifest when they enter the cell nucleus (Samadian et al., 2020). Notably, a specific genotoxicity mechanism of CNTs involves microtubule mimicry and disruption of the mitotic spindle functionality (Sargent et al., 2012; Siegrist et al., 2014). Further, it is widely acknowledged that CNT induce an increase in free radicals within animal tissues and cells (Shvedova et al., 2012; Møller et al., 2014). Experiments conducted both *in vivo* and *in vitro* have demonstrated the potential profibrogenic activity of CNTs (Dong and Ma, 2019; He et al., 2011; Manke et al., 2014; Mercer et al., 2013; Mishra et al., 2012; Shvedova et al., 2005; Snyder-Talkington et al., 2016; Vietti et al., 2016; Wang et al., 2011; Wang et al., 2015). Accumulating evidence indicates a close relationship between fibrosis and carcinogenesis (Dong and Ma, 2019), suggesting that this pathological scenario can also be considered as a mechanism parallel to genotoxicity potentially leading to carcinogenesis.

Earlier, our group explored the adverse effects of pristine MWCNT Taunit-M in concentrations relevant to occupational exposure through *in vitro* and *in vivo* experiments, as well as in an epidemiological study. Investigations conducted on mice have provided evidence of the fibrogenic potential of MWCNT Taunit-M (Khaliullin et al., 2015b). In concordance with these findings, the epidemiological study utilizing a bioinformatics approach has revealed an augmented likelihood of fibrogenic and carcinogenic events in workers who were occupationally exposed to MWCNT (Fatkhutdinova et al., 2016; Shvedova et al., 2016).

In this particular study, three commercially available CNTs with distinct physicochemical characteristics were chosen as the focal point of study; specifically, Taunit-M multi-walled carbon nanotubes, as well as pristine and purified TUBALL™ single-walled carbon nanotubes. All selected CNTs possess a high level of industrial production (Predtechenskiy et al., 2022a; Predtechenskiy et al., 2022b; Tkachev et al., 2013) and require elaborate study of toxicity and potential genotoxic effects.

The aim of our study was to evaluate and compare the genotoxic effect and mechanisms of DNA damage under exposure to Taunit-M MWCNT and TUBALL™ SWCNT in cells of the human respiratory system.

2. Materials and methods

2.1. Test materials

Pristine and purified from metal impurities single-walled carbon nanotubes TUBALL™ (manufacturer - OCSiAl Group Company) and multi-walled carbon nanotubes Taunit-M (manufacturer - NanoTechCenter LLC) were used as the material for the study. The physicochemical characteristics of the materials used are presented in Table 1.

2.2. Preparation and characterization of CNT dispersion

Biocompatible CNT dispersions were prepared following the same protocol employed in previously published studies (Timerbulatova et al., 2020). Briefly, CNTs were suspended in Dulbecco's modified Eagle's medium (DMEM) (PanEco, S410P, Russia) supplemented with 10% fetal bovine serum (BioSera, France) and antibiotics penicillin and streptomycin (25,000 U and 25,000 μg, 100-fold lyophilized preparation, PanEco, Russia). Stock dispersions with a concentration of 200 μg/ml were sonicated in a biological safety cabinet using Sonic Vibra Cell Sonicator (Sonics&Materials, USA) at the following operating parameters: 750 W, 20 kHz, 40% amplitude, pulse 5/6, time 30 min (Timerbulatova et al., 2020); other concentrations were obtained by dilution.

The characteristics of biocompatible stock dispersions were evaluated by dynamic light scattering (DLS) (Zetasizer Nano-ZS analyzer, Malvern Instruments, UK) and transmission electron microscopy (Hitachi HT7700 Exalens, Japan). Each sample was analyzed at least three times, with one measurement consisting of 15 repetitions of 10 s each.

CNT suspensions and vehicle medium were tested for the presence of bacterial endotoxin using the LAL reagent (lyzed amoebocytes from *Limulus Polyphemus*) (Endosafe KTA, series K2422L) by the kinetic turbidimetric method (State Pharmacopoeia of the Russian Federation, 2018).

2.3. Cell culture and treatments

Three immortalized cell lines, originating from the human respiratory system, were selected as cell models: two cell lines modeling epithelial cells of respiratory system, such as human bronchial epithelium cell line BEAS-2B (Cell Applications, Inc., USA) and human lung adenocarcinoma cell line A549 (CLS Cell Lines Service, Germany), and SV40-transformed cells from diploid human lung fibroblasts MRC5 representing stromal cells (cells kindly provided by Dr. Chernyak B.V., A.N. Belozersky Research Institute of Physical Chemistry, Moscow State University). Cells were cultured in DMEM with 10% fetal bovine serum and antibiotics penicillin and streptomycin; grown in a humidified atmosphere, with 5% CO_2, at 37 °C; seeded in cell culture dishes or 96-well plates depending on the assay and allowed to adhere for 48 h before the experiments.

Data on the CNT content in the air of the working area of enterprises producing the studied nanomaterials were used to calculate the lowest limit of concentration for *in vitro* experiments. The concentrations of SWCNTs at various production sites of the manufacturing enterprise

Table 1
Physico-chemical characteristics of purified and unpurified SWCNTs and MWCNT.

Physico-chemical characteristics *	Pristine SWCNT TUBALL™	Purified SWCNT TUBALL™	MWCNT Taunit-M
Metal impurities, %	14 ± 1 (Fe)	<1 (Fe)	<5 (Co)
Length, μm	>5	>5	>2
Average CNT diameter, nm	1.6 ± 0.4	1.6 ± 0.4	8–15
Total surface area, m^2/g	410	490	300–320

* as provided by the manufacturers.

were much lower than the reference level provided by the National Institute for Occupational Safety and Health of the USA (NIOSH Current Intelligence Bulletin 65, 2013), *i.e.* 1 μg/m^3 (REL NIOSH): the highest 8-h TWA air concentration of SWCNT TUBALL™ estimated by the surface-enhanced Raman spectroscopy (Dresselhaus et al., 2005) was <5% of REL NIOSH. As for the MWCNT production site, the 8-h TWA EC concentrations (respirable size fraction) were in the range of 0.7–1.3 μg/m^3 except for one workplace with a concentration of 2.8 μg/m^3 (Fatkhutdinova et al., 2016). Using CNT aerosol mass concentration of 1 μg/m^3 [NIOSH REL] and considering the simulated deposition in the alveolar zone of the human respiratory tract by the MPPD software (Multiple Path Particle Dosimetry V3.04), we calculated the deposited dose of CNT in human lungs over 25 years of work (250 shifts per year) with subsequent recalculation per 1 cm^2 of human alveolar epithelium and calculation of the required administered doses and concentrations (taking into account the area and volume of the plate well) for introduction into cell cultures. The calculated deposited dose in the lungs was 2000 μg, which corresponded to the concentration of 0.0006 μg/ml; the upper concentration limit was chosen as 200 μg/ml (Timerbulatova et al., 2021).

2.4. Cytotoxicity

The cytotoxicity of CNTs was determined by the MTS assay (Promega, USA), evaluating the metabolic activity and viability of cells, and the LDH assay (LDH Assay Kit, Abcam, UK), evaluating the integrity of the plasma membrane. For the MTS assay, cells were incubated with 18 concentrations from 0.0006 to 200 μg/ml for each type of CNTs studied over a 72-h period. Considering interference in formazan-based cytotoxicity assay caused by nanoparticles, each well plate was rinsed with PBS to remove the remaining carbon nanotubes before adding reagents for MTS assay (Esfandiary et al., 2014). The optical density of the samples in 3 replicates was assessed using Multiskan™ FC Microplate Photometer (Thermo Fisher Scientific, USA) at the wavelength of 492 nm. When analyzing the results of the MTS test, CNTs were considered to have the cytotoxic potential shown on this cell type when the viability of the cell culture decreased to <70% compared to the control, for which the viability was set to conditionally equal to 100% (ISO 10993-5:2009).

For the LDH assay, cells were exposed to four concentrations of each CNT type (100, 50, 0.03, and 0.0006 μg/ml) for 72 h. Considering the suspected interference, preliminary experiments were carried out in a cell-free medium; no interference was detected (Fig.S4-S6). LDH activity was determined in the supernatant of cells exposed to CNTs. After cells were exposed to CNT, the medium was collected and centrifuged. The supernatant was diluted by buffer at a ratio of 1:25 and assayed following the manufacturer's instructions. Cells without CNT exposure were used as negative controls and cells exposed to 1% Triton X-100 were used as positive controls for cytotoxicity. The optical density of the samples in 3 replicates was determined on Multiskan™ FC Microplate Photometer (Thermo Fisher Scientific, USA). The measurements were carried out every 10 min for 1 h in total; LDH activity was calculated from the change in the amount of NADH between 20 and 50 min. The change in LDH activity in the samples was calculated by taking into account the results for positive and negative controls using the following equation (Ursini et al., 2014):

$$\text{Cytotoxicity}, \% = (\text{mean (cells exposed to CNT)} - \text{mean(control)}) / (\text{mean(positive control)} - \text{mean(control)}).$$

2.5. Comet assay

The DNA comet assay is a sensitive method for studying single-stranded and double-stranded breaks, DNA oxidation, and alkylation, which has shown its effectiveness and is widely used in assessing the genotoxicity of nanomaterials (Azqueta and Dusinska, 2015; Di Ianni et al., 2021; García-Rodríguez et al., 2019). Genotoxicity was assessed using the alkaline variant of DNA comet assay (Trevigen, USA). Two concentrations of CNT (20 and 0.0006 μg/ml) were studied in the experiment at an exposure time of 72 h. 1 mM/ml doxorubicin was used to initiate DNA damage and untreated cells were used as a negative control. A suspension of incubated cells at a concentration of at least 2×10^5 cells/ml was mixed with low-melting agarose in a ratio of 1:10 and applied to glasses. Further manipulations with the micropreparation included the stages of lysis, alkaline denaturation, electrophoresis, and fixation according to the assay manufacturer's instructions. The micropreparations were stained with SybrGreen fluorescent dye (Invitrogen, USA), and comets were visualized using a fluorescent microscope (Olympus BX63, Japan) at a wavelength of 425–500 nm. Digital images were analyzed using the CaspLab software (v.1.2.3), assessing at least 100 randomly selected comets per micropreparation. The results were expressed as the percentage of DNA in the comet tail (% DNA in the comet tail).

2.6. TEM analysis

Subcellular localization of nanoparticles in cells was analyzed by transmission electron microscopy after incubation of cells with 100 μg/ml CNT dispersion over a 72 h period. The samples were fixed successively in glutaraldehyde and osmium tetroxide, dehydrated, and polymerized into Epon epoxy resin (Electron Microscopy Sciences, USA). Using a Leica UC7 ultramicrotome (Leica, Germany), sections of samples with a thickness in the range of 50–80 nm were obtained. Sections were then sequentially stained with saturated aqueous uranyl acetate and lead citrate on copper meshes with a Formvar/Carbon backing. Samples were visualized using a Hitachi HT 7700 Exalens transmission electron microscope (Hitachi, Japan).

2.7. Determination of reactive oxygen species (ROS)

Intracellular ROS were detected by 2,7-dichlorofluorescein diacetate (DCFH-DA) assay using the Cellular Reactive Oxygen Species Assay Kit DCFDA (Abcam, UK). Five concentrations of CNT (100, 50, 20, 0.03, 0.0006 μg/ml) were studied in three types of cell cultures after 72 h exposure. Tert-butyl hydroperoxide (TBHP) was used as a positive control, and untreated cells were used as a negative control. Fluorescence of the samples in 3 replicates was measured at 485/535 nm using a Varioskan LUX microplate reader (Thermo Fisher Scientific, Germany). The level of ROS was expressed as a fold increase relative to the negative control.

2.8. Gene expression

TGF-β1 stands out as a profibrotic marker and is widely studied in experiments *in vivo* and *in vitro* when assessing the toxicity of CNTs (Manke et al., 2014; He et al., 2011; Mishra et al., 2015; Wang et al., 2011; Wang et al., 2015). The mRNA levels of the *TGFB1* gene were assessed in cells exposed to 4 concentrations (100, 50, 0.03, 0.0006 μg/ml) of all types of CNT after 72 h exposure. Total RNA was obtained from cell suspensions by the phenol-chloroform extraction method using the TRIzol™ reagent (Invitrogen, USA). The resulting mRNA samples were stored at −20 °C. The quality and quantity of the isolated RNA were

Table 2
- Nucleotide sequence of specific primers and annealing temperature conditions.

Gene	Primer sequence (from 5′ to 3′)		Annealing temperature, °C
	Forward	Reverse	
TGFB1	GCT GAG GTA TCG CCA GGA AT	TAC CTG AAC CCG TGT TGC TC	55.5
GAPDH	GAC CAC AGT CCA TGC CAT CA	TCC ACC ACC CTG TTG CTG TA	63

assessed using Nanodrop Lite (ThermoFisher, USA). The subsequent cDNA synthesis was carried out using the MMLV RT kit (Evrogen, Russia) according to the manufacturer's instructions. The mRNA level was assessed by real-time PCR. To assess *TGFB1* gene expression, experiments were carried out in which the number of cycles and the annealing temperature of the primers varied. Amplification conditions and primer sequences are shown in Table 2. The *GAPDH* housekeeping gene was used as a reference gene. The synthesis of oligonucleotide primers, according to the given sequences, was carried out at Evrogen (Russia). Amplification of obtained cDNA was carried out using a commercial mixture for PCR 5× qPCRmix-HS SYBR (Evrogen, Russia) and a thermal cycler CXF96 (BioRad, USA) with following conditions: denaturation at 96 °C for 3 min; further 40 cycles, including denaturation at 96 °C for 10 s, annealing and visualization according to the selected annealing temperatures for each primer, and melting to evaluate the reaction. Each sample was performed in three repetitions. The level of gene expression was calculated using the $2^{-\Delta\Delta Ct}$ method relative to the control for each cell line (Livak and Schmittgen, 2001). Results of gene expression were reported as log2 fold change.

2.9. Statistical analysis

All experiments were repeated independently at least three times. All numerical values are represented as the mean ± SD. Microsoft Excel 2016 and R software (v.4.2.3) were used for figures and statistical processing. The Student's *t*-test was employed to compare the two groups in terms of cytotoxicity, ROS levels, and gene expression. The outcomes of the DNA comet assay were evaluated using the Kruskal-Wallis test. Additionally, multiple linear regression analysis with a backward procedure was performed to examine the impact of various CNT-related factors on the DNA damage level and *TGFB1* gene expression. CNT type, concentration, and ROS level were used as factors in regression models, while DNA in the comet's tail or *TGFB1* expression - as outcomes. Differences were considered statistically significant at *p*-values <0.05. For the MTS assay, an additional criterion was used, *i.e.*, only the reduction of cell viability below 70% was considered significant (ISO 10993-5:2009, 2009).

Table 3
Size distribution of CNT agglomerates (DLS) and bundles (TEM) in dispersions based on the DMEM culture medium supplemented with 10% FBS according to DLS and TEM results.

CNT type	DLS results	TEM results	
	Average size of CNT agglomerates, nm	CNT outer diameter, nm	CNT length, um
MWCNT	242.37 ± 3.11	12.90 ± 2.60	0.49 ± 0.06
Pristine SWCNT	604.4 ± 23.07	12.99 ± 1.12	1.38 ± 0.29
Purified SWCNT	847.43 ± 27.30	12.65 ± 3.15	1.33 ± 0.12

Results are reported as mean value ± standard deviation.

3. Results

3.1. Characterization of dispersed CNTs

The results of testing vehicle medium and CNT dispersions for the presence of bacterial contamination demonstrated an acceptable level of bacterial endotoxins (below 0.01 EU/ml), which confirmed the correctly chosen mode of processing the materials and observance of the conditions preventing the contamination of dispersions being prepared.

Dynamic light scattering (DLS) revealed the presence of CNT in stock suspensions in two distinct forms: agglomerates and bundles. Table 3 provides details regarding the average size of the agglomerates and the morphometric characteristics of CNT bundles. In all three CNT types, the primary peak was observed within the range of 100 to 1000 nm. Furthermore, for MWCNT and pristine SWCNT, a secondary peak was identified within the range of 1000 to 10,000 nm. The average size of MWCNT agglomerates in dispersions was several times smaller in size than those of both types of SWCNTs. DLS results are shown in Supplementary materials (Fig.S1-S3).

Transmission electron microscopy (TEM) was used to obtain images of individual nanotubes, bundles, and clusters of CNT in biocompatible dispersions (Fig. 1). MWCNT appeared as individual carbon nanotubes, while SWCNTs were often observed to form bundles and agglomerates. In addition, metallic impurities were visualized in pristine SWCNT but not in purified SWCNT. Morphometric characteristics of the carbon nanotubes in dispersions are shown in Table 3. The outer diameters of all CNTs under study were comparable, indicating the grouping of SWCNT into bundles. The length of bundles of purified and unpurified SWCNTs was similar, while the length of MWCNTs was three times shorter. Nevertheless, the measured average length of both MWCNT and pristine SWCNT bundles, as visualized in the dispersion, was found to be shorter than the specifications provided by the manufacturer. This discrepancy can be attributed to the tendency of nanotubes to adhere to each other and undergo twisting, which is inherent to their flexible structure.

3.2. Cytotoxicity of CNTs

Determination of the cytotoxic range is necessary for studies of the genotoxicity of nanomaterials to avoid false positive results when assessing genotoxic effects. Previously, we showed cytotoxic effects of pristine SWCNT and MWCNT in concentrations of 50–200 μg/ml and of purified SWCNT in the range of 25–200 μg/ml for BEAS-2B cells; there was no observed cytotoxicity from both SWCNT and MWCNT in A549 cells (Gabidinova et al., 2022).

The viability of MRC5-SV40 cells experienced a decline below 70% in response to MWCNT, starting at a concentration of 0.1 μg/ml (Fig. 2A), while cytotoxic concentrations resulting from exposure to SWCNT were higher, commencing from 6 μg/ml (Fig. 2B,C). Additionally, according to the results of the LDH assay, an increase in membrane permeability was observed at all concentrations of CNTs examined, including those corresponding to industrial exposures (Fig. 3).

3.3. Genotoxicity of CNTs

In bronchial epithelial cells, alveolar epithelial cells, and lung fibroblasts, exposure to all examined CNT types at a concentration of 0.0006 μg/ml, which corresponds to the upper limit of industrial exposure over a 72-h incubation period, did not result in a substantial elevation in the percentage of DNA in the tail in the comet assay (Fig. 4).

In BEAS-2B cell, exposure to CNTs at a concentration of 20 μg/ml led to a significant increase in the percentage of DNA in the tail (Fig. 4A). Although A549 cells exhibited no cell viability reduction up to a CNT concentration of 200 μg/ml, outcomes from the DNA comet assay demonstrated significant DNA damage upon exposure to all CNT types at a concentration of 20 μg/ml and higher, with the percentage of DNA in the tail in cells incubated with CNT being comparable to doxorubicine as

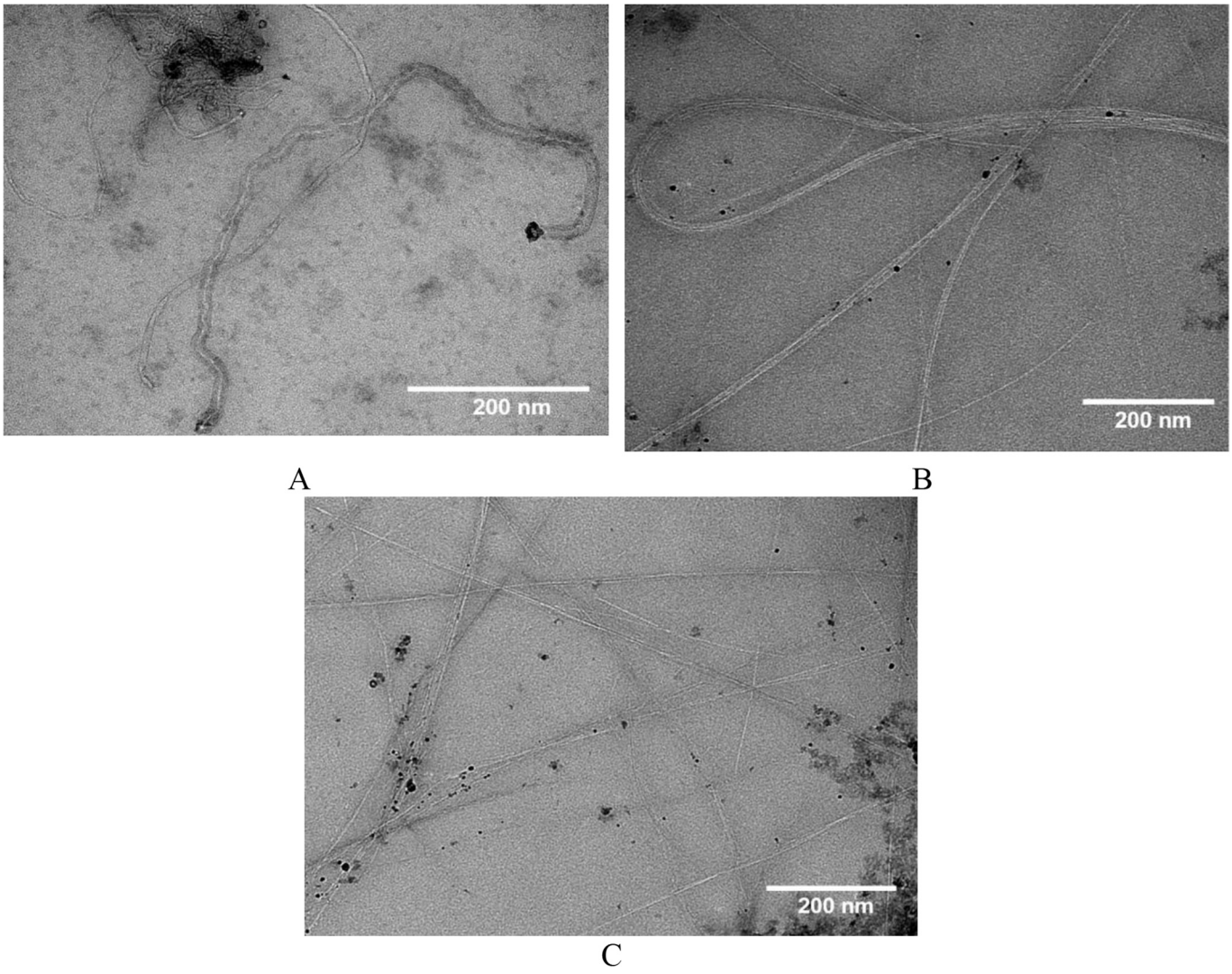

Fig. 1. TEM images of MWCNT (A), pristine SWCNT (B), and purified SWCNT (C) dispersions based on the DMEM culture medium supplemented with 10% FBS.

the positive control (Fig. 4B); all CNT exhibited a comparable DNA fragmentation level. Exposure of MRC5-SV40 cells to MWCNT and purified SWCNT at a concentration of 20 μg/ml for 72 h resulted in a notable increase in the percentage of DNA in the tail when compared to the control, whereas exposure to pristine SWCNT did not elicit a similar effect (Fig. 4C).

3.4. ROS in cells after CNT exposure

Evaluation of cellular ROS levels using the DCFH-DA test revealed a dose-dependent escalation in ROS levels within bronchial epithelial cells in response to all types of CNT, with a significant increase observed from a concentration of 20 μg/ml upwards (Fig. 5A). Notably, exposure to pristine SWCNT at a concentration of 20 μg/ml resulted in a higher level of oxidative stress in BEAS-2B cells compared to MWCNT and purified SWCNT ($p < 0.01$). However, at higher concentrations, this effect almost smoothed out. In A549 alveolar epithelial cells, a significant increase in ROS levels was also evident upon exposure to all CNTs at concentrations of 20, 50, and 100 μg/ml, and discrepancies in the ability of different CNTs to induce oxidative stress were more distinct (Fig. 5B). Pristine SWCNT exhibited an over twofold increase in ROS levels compared to MWCNT, even at higher concentrations ($p < 0.05$). Similar results to those observed in the A549 cell culture were obtained in MRC-SV40 fibroblasts (Fig. 5C).

3.5. The effect of ROS on DNA damage in cells after CNT exposure

Multiple linear regression models were built to assess the effect of the level of reactive oxygen species on DNA damage upon exposure to different types of CNTs. Initially, the type of CNT, CNT concentrations, and the level of oxidative stress were chosen as independent variables. Table 4 presents the regression models linking CNT concentration, CNT type, ROS level, and the percentage of DNA in the comet tail for each cell line. Exposure of all types of cells to all types of CNT under study was linked to a higher percentage of damaged DNA compared to the control, but the mechanisms involved were different. The findings of the study demonstrated that an elevation in ROS level corresponded to an increase in the percentage of damaged DNA in BEAS-2B and A549 epithelial cells. Moreover, ROS production seemed to be the mechanism that best explains the DNA damage in BEAS-2B cells exposed to MWCNT. SWCNT increased the DNA fragmentation in BEAS-2B cells, not being dependent on the level of oxidative stress. For A549 cells, the dose along with ROS production, regardless of the type of CNT, were parameters increasing the percentage of damaged DNA. Conversely, contrasting outcomes were observed for MRC5-SV40 fibroblasts in comparison to epithelial cells. Specifically, an increase in the concentration of CNT also correlated with an increase in DNA damage, but an inverse association with the level of ROS was found. At the same concentrations, MRC5-SV40 fibroblasts were less sensitive to MWCNT than to SWCNT exposure.

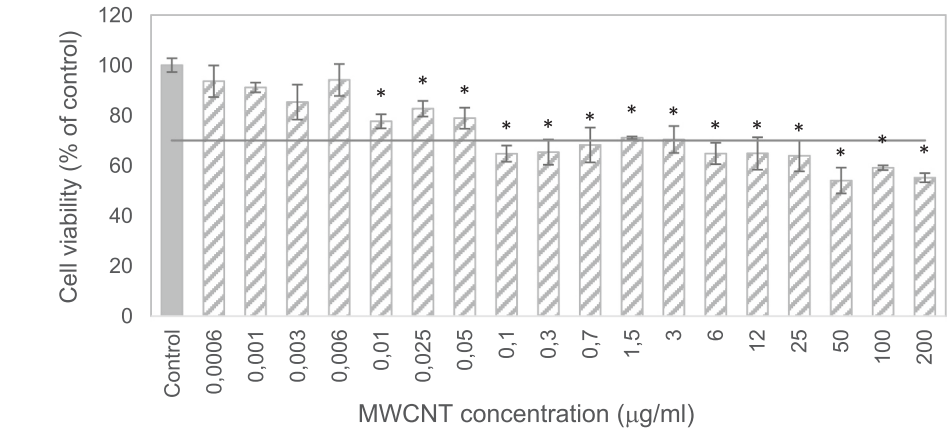

A

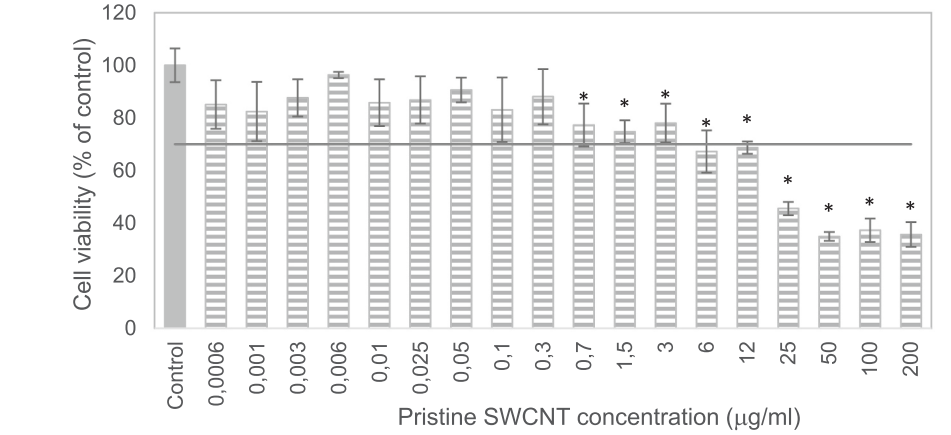

B

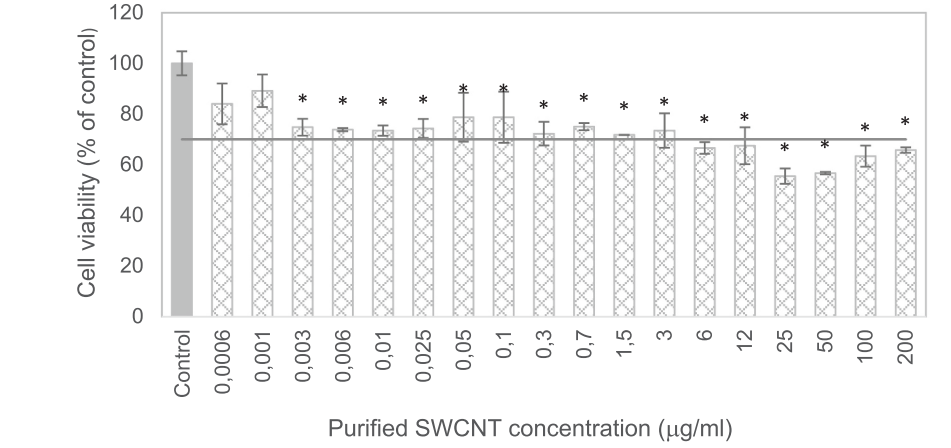

C

Fig. 2. MTS assay: MRC5-SV40 cell viability after 72-h exposure to MWCNT (A), pristine SWCNT (B), purified SWCNT (C); mean value ± standard deviation of metabolic activity of cells. The threshold line indicates a level of 70% cell viability. * - $p < 0.05$ compared to control.

Thus, a schematic summary of the processes that can lead to DNA damage when exposed to CNT is presented in Supplementary Materials (Table S1).

3.6. CNT interaction with cells

We successfully demonstrated the interaction of MWCNT with the nuclear membrane of A549 cells (Fig. 6). Nanoparticles formed clusters near the nuclear membrane and traversed its barrier. Single MWCNT were even found within the nucleus, suggesting a potential direct impact of this type of CNT on DNA (Fig. 6).

Similar results were obtained in MRC5-SV40 fibroblasts: all CNTs also penetrate cells, while MWCNT tend to form clusters in the cytoplasm of cells (Fig. 7). Single MWCNT penetrating the nuclear membrane of MRC5-SV40 cells were found (Fig. 8).

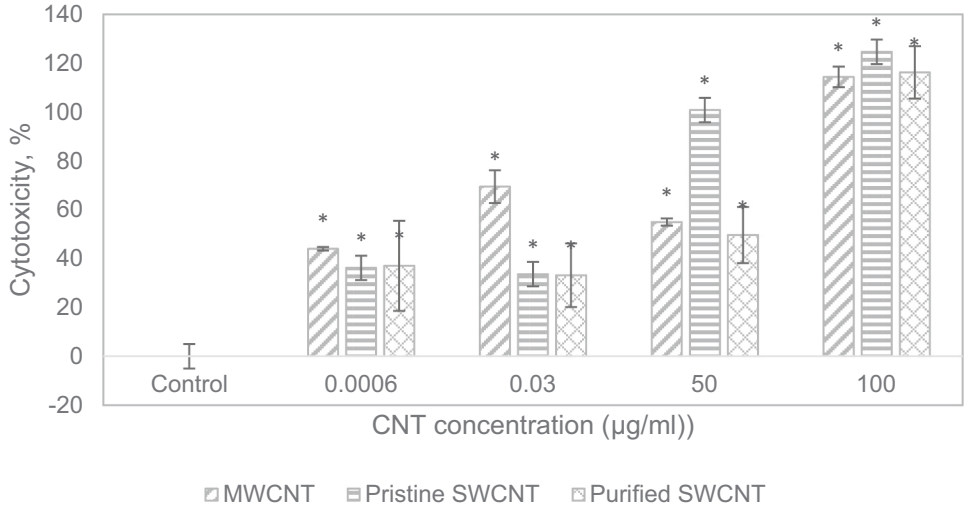

Fig. 3. LDH assay: Cytotoxicity in MRC5-SV40 cells after 72-h exposure to MWCNT, pristine SWCNT, purified SWCNT; mean value ± standard deviation. * - $p < 0.05$ compared to control.

3.7. TGFB1 expression upon exposure to CNTs

When assessing the gene expression related to fibrosis in bronchial epithelial cells, it was observed that exposure to MWCNT at concentrations of 0.0006 and 0.03 μg/ml for 72 h led to upregulation of the *TGFB1* gene in BEAS-2B cells – $p < 0.05$ for comparison with the control (Fig. 9); at higher concentrations *TGFB1* gene was comparable with the control. Opposite trends were observed for two types of SWCNT, with an increase in *TGFB1* gene expression at a concentration of 100 μg/ml ($p < 0.05$ for comparison with the control for pristine SWCNT), preceded by a decrease in *TGFB1* gene expression at lower concentrations. In A549 alveolar epithelial cells, positive expression of the *TGFB1* gene was observed upon exposure to CNTs at all concentrations ($p < 0.05$ for all comparisons with the control) (Fig. 10). In MRC5-SV40 fibroblasts, expression of the *TGFB1* gene in cells exposed to all types of CNT did not differ from the control, except downregulation of *TGFB1* gene upon exposure to pristine SWCNT at a concentration of 0.0006 μg/ml (Fig. 11).

Table 5 shows multiple linear regression models relating independent variables such as ROS level, CNT concentration, and CNT type to the level of *TGFB1*gene expression in three cell lines. BEAS-2B cells exposed to MWCNT showed the highest level of *TGFB1* gene expression compared to both types of SWCNT at all concentrations under study; a negative correlation of *TGFB1* gene expression to the level of ROS production was revealed. In contrast, in A549 cells, the level of *TGFB1* gene expression was positively correlated with oxidative stress, regardless of the type of CNT. According to the linear regression model considering not only CNT types but other parameters, expression of the *TGFB1* gene in MRC5-SV40 fibroblasts exposed to MWCNT was significantly lower compared to the control. A summary of different CNT-related factors increasing the *TGFB1* gene expression in three types of cells is demonstrated in Supplementary materials (Table S2).

4. Discussion

The genotoxic potential of three different types of industrial CNTs in human respiratory system cells has been investigated. Before examining the genotoxic effects of the materials, an essential preliminary stage involves assessing cytotoxicity (Kohl et al., 2020). Due to the potential interference that may arise with DNA break detection methods, it is advised to conduct comet DNA assay at non-cytotoxic concentrations (Kohl et al., 2020). To estimate the cytotoxicity range, two distinct tests, namely the MTS assay and the LDH assay, which evaluate different mechanisms of toxicity, were applied. In our previous research, we observed cytotoxic effects at high concentrations (50–200 μg/ml) in BEAS-2B cells and no cytotoxic effects induced by CNTs in A549 cells (Gabidinova et al., 2022). The latest results revealed cytotoxicity at all concentrations studied (the LDH assay) in MRC5-SV40 human lung fibroblasts.

Currently, a specific threshold for cytotoxicity that results in interference with genotoxicity assessment has not been established. One of the reasons contributing to this absence of consensus is the utilization of different cytotoxicity assessment methods. The recommended limit of 25% cytotoxicity has been suggested, and it has been reported that DNA fragmentation does not impact the results of the DNA comet assay in samples with a cell viability decrease of <45% (Azqueta et al., 2022). Hence, in our study, we set the endpoints of the genotoxicity investigation at concentrations of 0.0006 μg/ml and 20 μg/ml. The first concentration aligns with the reference level proposed by the US NIOSH of 1 $\mu g/m^3$ (REL NIOSH). Exposure to CNT at this concentration did not result in a decrease in cell viability of >25%, according to the MTS test in any of the cell cultures examined. The second subtoxic concentration was chosen such that the cell viability, determined by the MTS test, was at least 55%.

Our results from the DNA comet assay demonstrated no genotoxic effects of the CNT at the concentration corresponding to industrial exposures (0.0006 μg/ml). However, an increase in the number of unstable DNA regions was observed at the subtoxic concentration of CNT equal to 20 μg/ml. Previous studies that investigated the genotoxicity of different types of CNT at concentrations mainly higher than those utilized in our study have yielded inconsistent results. These discrepancies might arise from variations in cell sensitivity to CNT (Di Ianni et al., 2021; Lindberg et al., 2013; Louro et al., 2016; May et al., 2022) and the physicochemical characteristics of the CNT under investigation (Di Giorgio et al., 2011; Louro et al., 2016; May et al., 2022; Møller et al., 2021; Öner et al., 2018; Siegrist et al., 2019; Wils et al., 2021a).

The next step of our study was to investigate the mechanisms by which various types of CNT induce genotoxic effects in cells of the human respiratory system. Oxidative stress (Di Giorgio et al., 2011; Fukai et al., 2018; He et al., 2012; Shvedova et al., 2012; Wils et al., 2021a; Wils et al., 2021b), direct interaction of CNT with genetic material (Di Giorgio et al., 2011; Öner et al., 2018), cellular transformation, and fibrogenic effects (He et al., 2012; Polimeni et al., 2016; Vales et al., 2016; Ventura et al., 2022; Wang et al., 2010) have been proposed as possible mechanisms contributing to the potential genotoxicity and carcinogenicity of CNT.

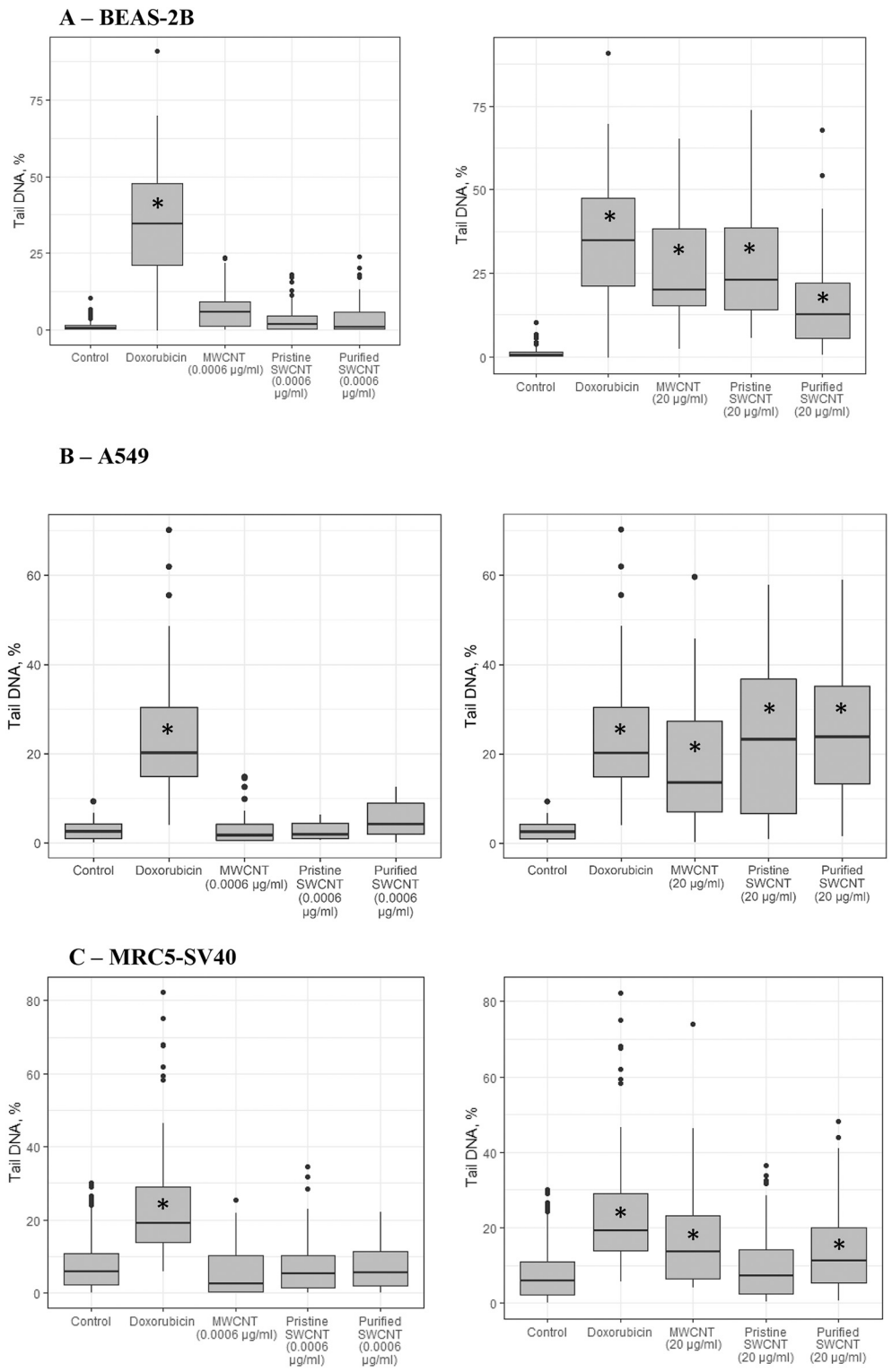

Fig. 4. The percentage of DNA in the comet tail in cells BEAS-2B (A), A549 (B), MRC5-SV40 (C) according to the results of the DNA comet assay after 72-h exposure to CNT; mean value ± standard deviation. * - $p < 0.05$ in comparison with the control.

The generation of free radicals is widely recognized as the primary mechanism underlying genotoxicity (van Berlo et al., 2012; Samadian et al., 2020). Our experimental findings, as determined through DCFH-DA assay, revealed a noteworthy increase in intracellular ROS production following 72 h of exposure to all types of CNT, beginning at a concentration of 20 μg/ml. Regression analysis further exhibited a positive correlation between DNA damage and oxidative stress levels in respiratory epithelial cells upon exposure to CNT at a concentration of 20 μg/ml upwards. However, a direct relationship was not observed for human lung fibroblasts, indicating the potential activation of distinct mechanisms of CNT genotoxic effects in different cell types. While in epithelial cells ROS production might play a direct role in increasing the number of cells with DNA fragmentation, in human lung fibroblasts exposure to CNT seemed to block ROS-depended cell regulatory

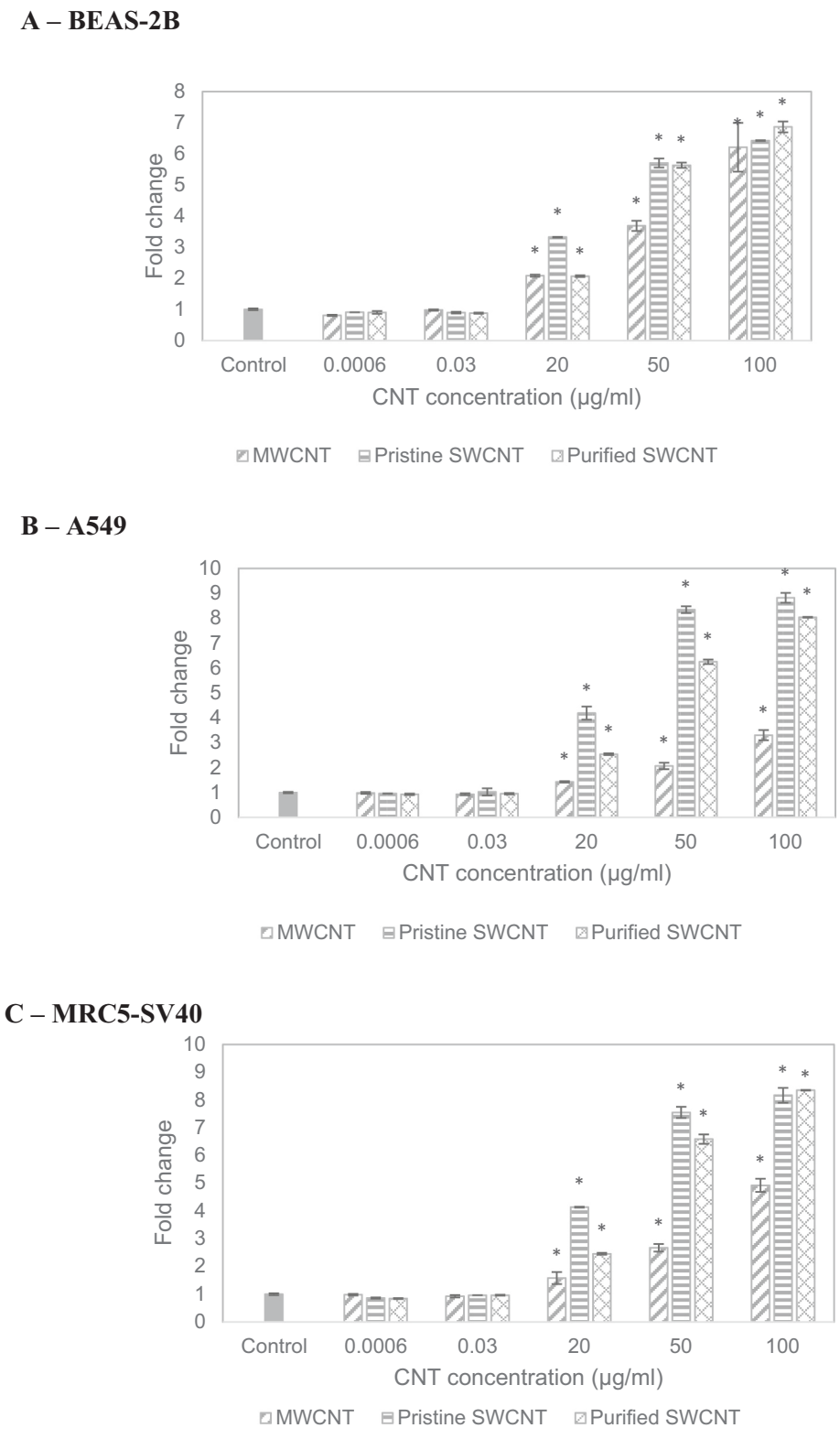

Fig. 5. Fold change of ROS level compared to control in cells BEAS-2B (A), A549 (B), MRC5-SV40 (C) in DCFH-DA assay after 72-h CNT exposure; mean value ± standard deviation. * - $p < 0.05$ in comparison with the control.

pathways. Similar observations of increased free radical production and genotoxic effects resulting from CNT exposure have been reported by other research groups across various cell types, including FE1-MML mouse lung epithelial cells, BEAS-2B human bronchial epithelial cells, MCL-5 lymphoblastoid cells, RAW264.7 mouse macrophages, L929 mouse fibroblasts, and human peripheral blood lymphocytes (Alarifi and Ali, 2015; Di Giorgio et al., 2011; Fraser et al., 2020; Fukai et al., 2018; Kim and Yu, 2014; Kim et al., 2015; Manshian et al., 2013; Migliore et al., 2010; Vales et al., 2016; Wils et al., 2021a). Meanwhile, these conclusions were based rather on qualitative than quantitative assessment. Notably, several studies have reported no direct association between increased free radical production and DNA damage, as assessed

Table 4
Multiple linear regression models: effects of CNT concentration, CNT type, and ROS level on the percentage of DNA in the comet's tail in three types of cells.

DNA in the comet's tail (%) in different cell lines / CNT related factors	Concentration, μg/ml (ß ± SE [CI 2.5%; 97.5%])	CNT type *vs* control (ß ± SE [CI 2.5%; 97.5%])			ROS level, fold change (ß ± SE [CI 2.5%; 97.5%])	ROS level × CNT type (ß ± SE [CI 2.5%; 97.5%])			R^2	p
		MWCNT	Pristine SWCNT	Purified SWCNT		MWCNT	Pristine SWCNT	Purified SWCNT		
BEAS-2B *	−0.06 ± 0.16 [−0.39; 0.25]	3.83 ± 2.68 [−1.43; 9.08]	**3.14 ± 1.47 [0.25; 6.03]**	**3.48 ± 1.56 [0.41; 6.56]**	**11.10 ± 1.81 [7.55; 14.65]**	**4.99 ± 1.91 [1.23; 8.74]**	–	–	0.46	<0.001
A549 **	**0.68 ± 0.10 [0.47; 0.87]**	–	–	–	**2.19 ± 0.87 [0.47; 3.91]**	–	–	–	0.32	<0.001
MRC5-SV40 ***	**0.59 ± 0.07 [0.46; 0.73]**	**−2.28 ± 1.12 [−4.49; −0.08]**	−1.35 ± 1.08 [−3.46; 0.76]	−1.76 ± 1.07 [−3.85; 0.34]	**−3.01 ± 0.64 [−4.27; −1.76]**	–	–	–	0.14	<0.001

ß ± SE – standardized regression coefficient ± standard error for CNT-related factors left in the model after backward procedure; CI 2.5%; 97.5% - confidence interval.
Full regression models for each cell type are presented below:
Variables shown in bold were considered statistically significant ($p < 0.05$).

* BEAS-2B: TailDNAPercentage = −9.99 + **11.10ROS_level** – 0.06Concentration + 3.83MWCNT + **3.14Pristine_SWCNT** + **3.48Purified_SWCNT** + **4.99ROS × MWCNT.**

** A549: TailDNAPercentage = 1.50 + **2.19ROS_level** + **0.68Concentration.**

*** MRC5-SV40: TailDNAPercentage = 11.22–**3.01ROS_level** + **0.59Concentration – 2.28MWCNT** − 1.35Pristine_SWCNT – 1.76Purified_SWCNT.

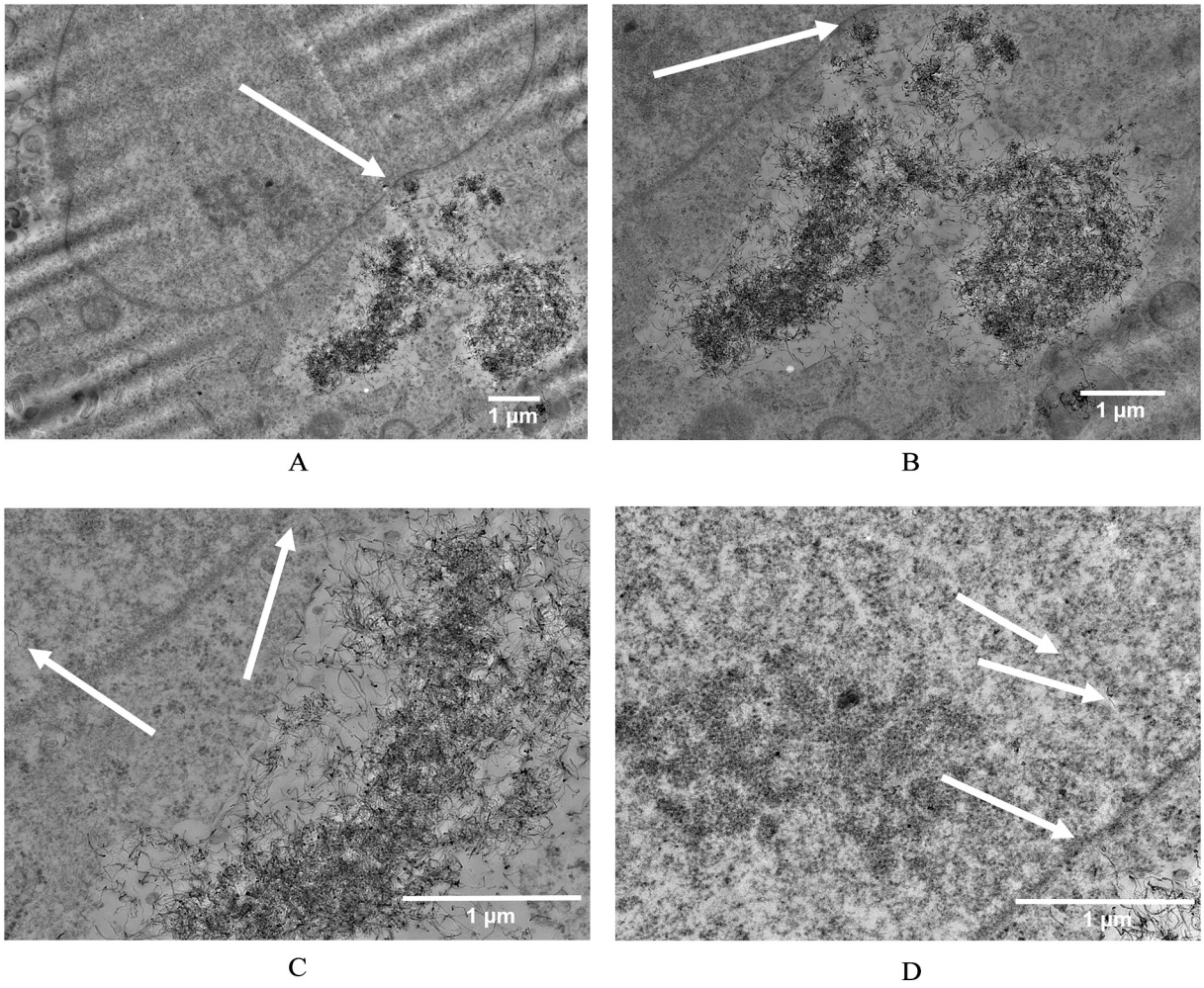

Fig. 6. Interaction of MWCNT with the nucleus of A549 cells at a concentration of 100 μg/ml after 72 h of exposure on images obtained by transmission electron microscopy. Images captured at different magnifications: A – x6, B – x10, C – x20, D – x20. Arrows indicate carbon nanotubes.

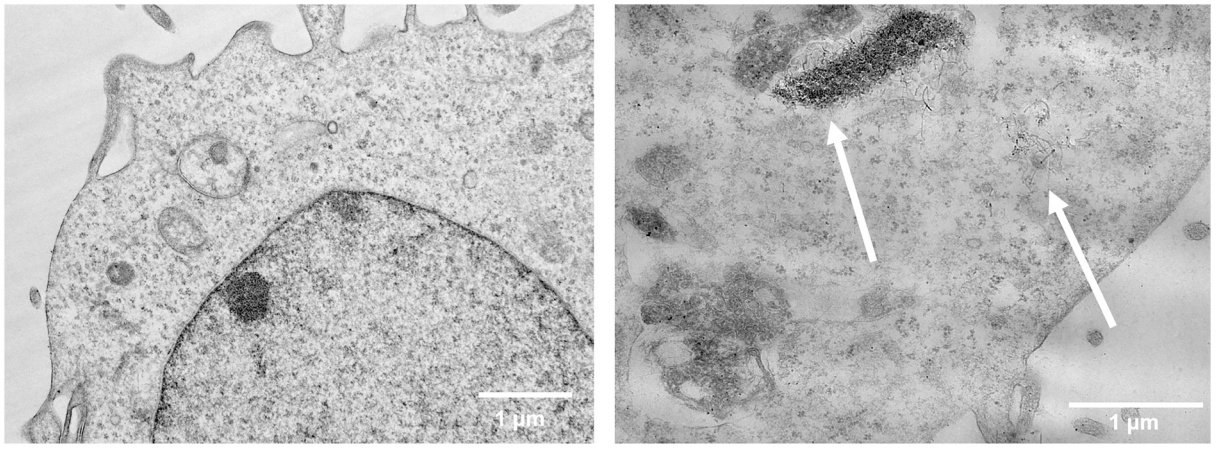

Fig. 7. TEM images of MRC5-SV40 cells: A – control without exposure, B – after 72 h of exposure to MWCNT at a concentration of 100 μg/ml. Arrows indicate carbon nanotubes.

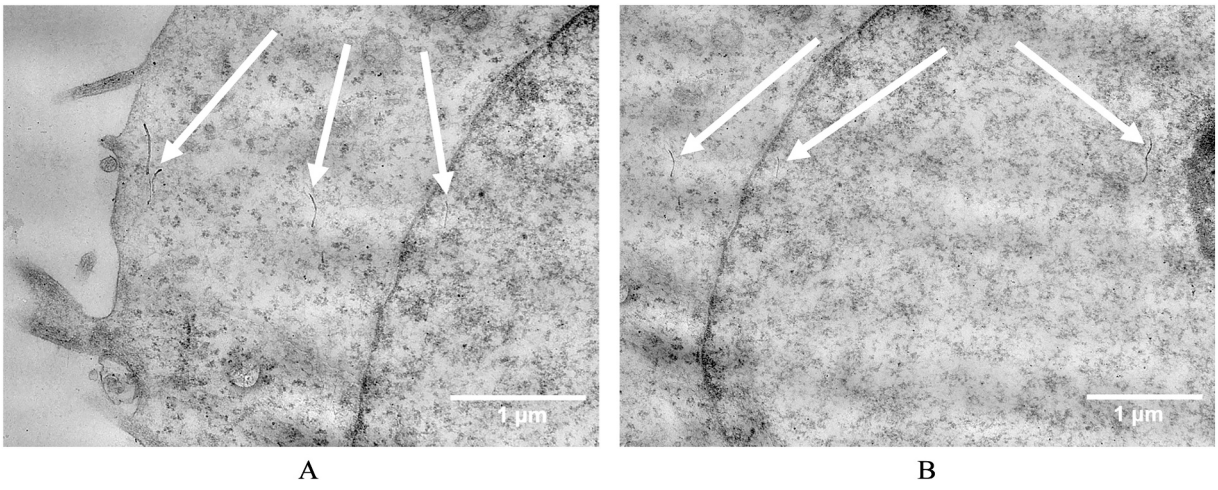

Fig. 8. Interaction of MWCNT with the nucleus of MRC5-SV40 cells at a concentration of 100 μg/ml after 72 h of exposure on images obtained by transmission electron microscopy. Images captured at different magnifications: A – x15, B – x12. Arrows indicate carbon nanotubes.

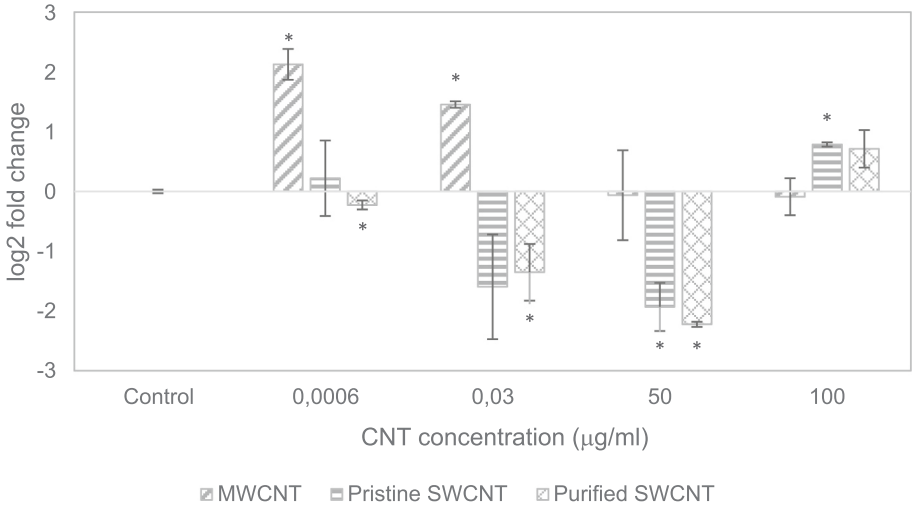

Fig. 9. Log2 fold change values for *TGFB1* gene expression in BEAS-2B cells after 72-h exposure to CNT: mean value ± standard deviation. * - $p < 0.05$ in comparison with the control.

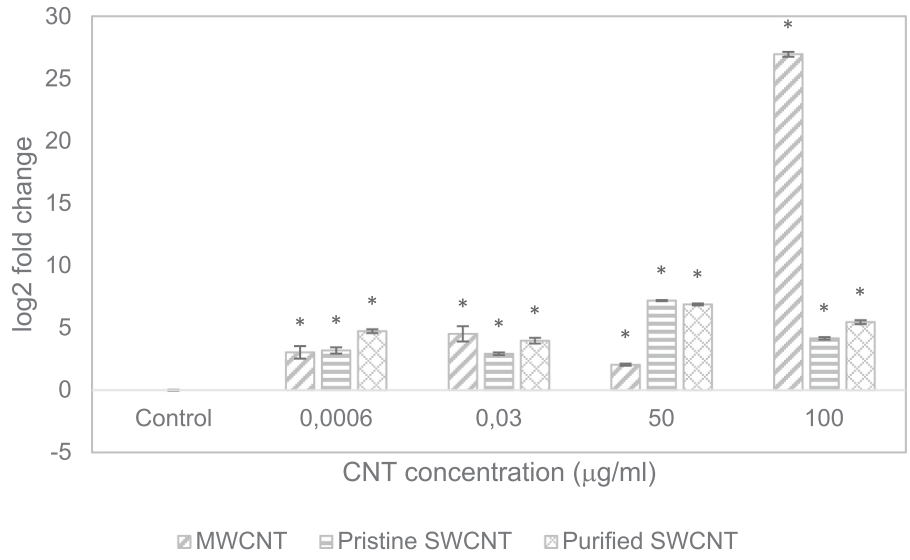

Fig. 10. Log2 fold change values for *TGFB1* gene expression in A549 cells after 72-h exposure to CNT: mean value ± standard deviation. * - $p < 0.05$ in comparison with the control.

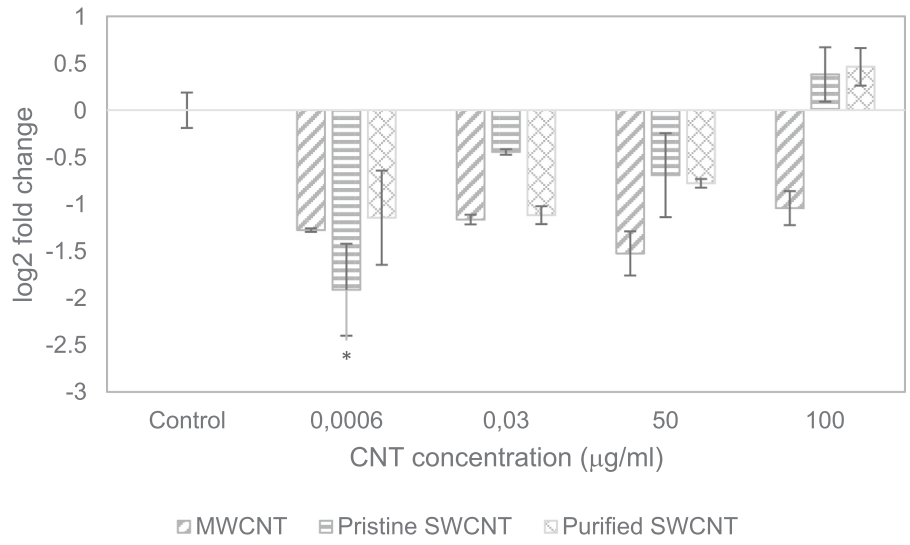

Fig. 11. Log2 fold change values for *TGFB1* gene expression in MRC5-SV40 cells after 72-h exposure to CNT: mean value ± standard deviation. * - $p < 0.05$ in comparison with the control.

through DNA comet assay, micronucleus test, and H2AX phosphorylation (Manshian et al., 2013; Vales et al., 2016). The data indicate that iron impurities present in CNT facilitate ROS formation through the metal-dependent Fenton reaction (Murray et al., 2009; Shvedova et al., 2003). Such disparities suggest the involvement of additional pathways, beyond oxidative stress, in the manifestation of CNT toxicity depending on different CNT-related factors.

We have demonstrated the features of uptake and deposition of CNT in the cells of the human respiratory system. Our previous investigations have provided evidence of CNT entry into the human bronchial and alveolar epithelial cells, revealing an inclination towards invagination of the cell membrane (Gabidinova et al., 2022). In the current study, MWCNT exhibited a propensity to accumulate near the nuclear membrane, raising the possibility of subsequent nuclear uptake, as confirmed by TEM. This direct mechanistic pathway of genotoxicity should be taken into consideration. Conversely, the intranuclear SWCNT uptake in human respiratory cells was not observed in our investigation. However, it is important to recognize that there were differences in cell uptake between MWCNT and SWCNT, as the latter did not form extensive intracellular accumulations. Other researchers have reported both MWCNT and SWCNT contact with the cell nucleus (Di Giorgio et al., 2011; Fujita, 2021; Öner et al., 2018; Sargent et al., 2012; Siegrist et al., 2014; Siegrist et al., 2019). Moreover, some of them used quantitative measurements (Öner et al., 2018; Siegrist et al., 2019). When considering the CNT uptake into the cellular nucleus, it is of utmost importance to clear up some concerns. The unique capability of CNT to disrupt the functionality of nuclear structures like microtubules and centrosomes was demonstrated (Sargent et al., 2012; Siegrist et al., 2014; Siegrist et al., 2019), although sufficient information is yet to be obtained for comprehensive characterization of the CNT associated with such capability. Subsequently, investigators face the challenge of quantitatively assessing the extent to which CNT penetrate the nucleus and elucidating the correlation between this parameter and their toxic properties. For instance, Öner et al. demonstrated that a greater deposition of SWCNT in the nucleus of 16HBE human bronchial epithelial cells subsequently induced greater genotoxicity when compared to MWCNT (Öner et al., 2018).

Our research also demonstrates that the investigated CNTs exhibit

Table 5
Multiple linear regression models: effects of CNT concentration, CNT type, and ROS level on the *TGFB1* expression in three types of cells.

TGFB1 gene expression in different cell lines / CNT related factors	Concentration, μg/ml (ß ± SE [CI 2.5%; 97.5%])	CNT type *vs* control (ß ± SE [CI 2.5%; 97.5%])			Concentration × CNT type *vs* control, (ß ± SE [CI 2.5%; 97.5%])			ROS level, fold change (ß ± SE [CI 2.5%; 97.5%])	ROS level × CNT type (ß ± SE [CI 2.5%; 97.5%])			R^2	p
		MWCNT	Pristine SWCNT	Purified SWCNT	MWCNT	Pristine SWCNT	Purified SWCNT		MWCNT	Pristine SWCNT	Purified SWCNT		
BEAS-2B *	0.04 ± 0.02 [−0.01; 0.10]	**10.66 ± 2.34 [3.22; 18.11]**	−0.28 ± 0.63 [−2.29; 1.74]	−0.43 ± 0.49 [−2.00; 1.14]	**0.44 ± 0.13 [0.02; 0.87]**	0.01 ± 0.02 [−0.08; 0.07]	–	−0.53 ± 0.27 [−1.39; 0.33]	**−9.09 ± 2.49 [−17.00; −1.18]**	0.04 ± 0.36 [−1.09; 1.18]	–	0.88	0.04
A549 **	−0.95 ± 0.48 [−2.09; 0.20]	34.13 ± 41.31 [−63.56; 131.82]	3.91 ± 41.41 [−94.01; 101.83]	24.82 ± 40.42 [−70.76; 120.40]	–	–	–	**19.97 ± 6.90 [3.66; 36.28]**	–	–	–	0.40	0.125
MRC5-SV40 ***	0.004 ± 0.005 [−0.007; 0.02]	**−0.77 ± 0.32 [−1.53; −0.003]**	−0.49 ± 0.32 [−1.25; 0.27]	−0.50 ± 0.32 [−1.25; 0.25]	–	–	–	0.02 ± 0.07 [−0.14; 0.18]	–	–	–	0.42	0.11

ß ± SE – standardized regression coefficient ± standard error for CNT-related factors left in the model after backward procedure; CI 2.5%; 97.5% - confidence interval.
Full regression models for each cell type are presented below:
Variables shown in bold were considered statistically significant ($p < 0.05$).

* BEAS-2B: TGFB1_expression_level = 1.53–0.53ROS_level + 0.04Concentration + **10.66MWCNT** – 0.28Pristine_SWCNT – 0.43Purified_SWCNT **– 9.09ROS × MWCNT** + 0.04ROS × Pristine_SWCNT + **0.44Concentration × MWCNT** – 0.01Concentration × Pristine_SWCNT.

** A549: TGFB1_expression_level = −18.97 + **19.97ROS_level** – 0.95Concentration + 34.13MWCNT – 3.91Pristine_SWCNT – 24.82Purified_SWCNT.

*** MRC5-SV40: TGFB1_expression_level = 0.98 + 0.02ROS_level + 0.004Concentration **– 0.77MWCNT** – 0.49Pristine_SWCNT – 0.50Purified_SWCNT.

profibrogenic properties in BEAS-2B and A549 epithelial cells. We observed an upregulation of *TGFB1* expression in bronchial epithelial cells at non-cytotoxic concentrations of MWCNT and high cytotoxic concentrations of pristine SWCNT. Regression analysis detected increased *TGFB1* expression in BEAS-2B bronchial epithelial cells after MWCNT exposure inversely depending on the ROS level. Similarly, all types of CNT at the studied concentrations induced an increased expression of a profibrotic factor in A549 cells, and this effect was dependent on the level of ROS generation. We observed that none of the three types of CNT upregulate *TGFB1* in MRC5-SV40 human fibroblasts. Moreover, expression of the *TGFB1* gene in MRC5-SV40 fibroblasts exposed to MWCNT was significantly lower compared to the control. These findings align with previous studies where exposure to MWCNT resulted in increased *TGFB1* gene expression in BEAS-2B cells (He et al., 2011; Mishra et al., 2012; Wang et al., 2011; Wang et al., 2015). The crucial role of oxidative stress in initiating fibrosis was also shown (Azad et al., 2013; Bargagli et al., 2009; Chakravarthy et al., 2018; Inghilleri et al., 2006; Ma, 2010). A number of studies have demonstrated that oxidative stress induced by CNT enhanced the production and activation of profibrotic factors, including TGF-β1 (He et al., 2011; Ma, 2010; Manke et al., 2014). Collectively, these findings emphasize the pivotal role of oxidative stress as a key regulator of CNT-induced fibrogenesis. However, in our study, we demonstrated a linear relationship only for A549 cells, while for other cell types, the relationship between ROS and *TGFB1* expression turned out to be more complicated.

Our findings also imply the potential contribution of multiple mechanisms in the induction of DNA damage upon exposure to various types of CNT. MWCNT are characterized by a range of mechanisms that result in genetic material damage, including direct exposure to CNT, high level of ROS, and increased expression of *TGFB1*. SWCNT exhibited genotoxicity comparable to MWCNT and possess a greater ability to generate ROS, regardless of the presence/absence of metal impurities; these findings come alongside those of Fraser et al. (2020). Pristine SWCNT, when present in high concentrations, induce an upregulation of *TGFB1* expression. However, despite previous studies demonstrating the penetration of SWCNT into the cellular cytoplasm (Gabidinova et al., 2022), we were unable to observe their entry into the cell nucleus. No direct quantitative relationship between DNA damage or *TGFB1* expression with the level of oxidative stress upon exposure to SWCNT was shown, which suggests that the genotoxic effects of SWCNT are dependent on their physicochemical properties and implies the involvement of alternative mechanisms such as apoptosis, ferroptosis, and reactive nitrogen species (RNS).

Previous *in vivo* and 2D *in vitro* studies hypothesized that epithelial cells inducing the production of TGF-β1 could trigger epithelial-mesenchymal transition and indirectly activate fibroblasts, leading to the release of growth factors and cytokines (Kalluri and Weinberg, 2009; Pardali et al., 2017; Polimeni et al., 2016; Vietti et al., 2016), ultimately contributing to fibrosis development. Our results revealed the increased expression of profibrotic factor *TGFB1* in epithelial cells, however, the application of monoculture without the presence of fibroblasts does not allow for verification of profibrogenic outcomes under CNT exposure. The findings obtained in the current study indicate the potential significance of applying advanced co-culture models, including 3D cell models, in modeling the interplay between epithelial cells and fibroblasts and studying their role in fibrogenesis.

The utilization of CNT dispersions containing predominantly agglomerated CNT can complicate the interpretation of toxicity results in dispersed nanotubes (Mercer et al., 2013; Sager et al., 2009). Mercer et al. demonstrated the ability of larger MWCNT particles to undergo dissociation, leading to the formation of smaller structures and individual CNT within the alveolar septa and subpleural lung tissue of mice (Mercer et al., 2013). In our study, we validated the presence of individual CNT within the targeted cellular entities, thereby suggesting the potential for disintegration of CNT agglomerates upon cellular entry. It should be noted that within 48 h, a major part (up to 85%) of the administered dose of CNT interact with cells (Septiadi et al., 2019). The features of CNT behavior in biological systems must be taken into account when planning and conducting toxicological experiments.

5. Conclusion

Results from the DNA comet assay demonstrated no genotoxic effects of the CNT on three cell lines (BEAS-2B human bronchial epithelial cells, A549 alveolar epithelial cells, MRC5-SV40 human fibroblasts) at concentrations corresponding to registered occupational exposures.

However, an increase in the number of unstable DNA regions was observed at subtoxic concentrations of CNT equal to 20 μg/ml, suggesting a dose-dependent genotoxicity of the materials.

ROur study revealed that CNT with different characteristics exert a comparable genotoxic potential, albeit through distinct mechanisms. MWCNT were found to penetrate the nucleus of respiratory system cells, potentially interacting directly with genetic material, as well as to enhance ROS production and *TGFB1* gene expression. For alveolar epithelial cells and fibroblasts, genotoxicity depended mainly on MWCNT concentration, while for bronchial epithelial cells – on their oxidative potential. Meanwhile, the mechanisms of SWCNT genotoxicity are not so obvious Oxidative stress and increased expression of profibrotic factors could not fully explain DNA damage under SWCNT exposure, and other mechanisms might be involved.

The enumeration of the quantity of MWCNT and SWCNT that successfully pass through the nuclear membrane of cells of the respiratory system and the juxtaposition of this parameter with the magnitude of DNA damage and levels of ROS and profibrotic factors has the potential to offer novel insights into comprehending the mechanistic underpinnings of the genotoxicity induced by various CNTs.

CRediT authorship contribution statement

Liliya M. Fatkhutdinova: Conceptualization, Methodology, Supervision, Writing – review & editing. **Gulnaz F. Gabidinova:** Conceptualization, Formal analysis, Investigation, Visualization, Writing – original draft, Writing – review & editing. **Amina G. Daminova:** Investigation, Visualization, Writing – review & editing. **Ayrat M. Dimiev:** Investigation, Resources, Writing – review & editing. **Timur L. Khamidullin:** Investigation, Writing – review & editing. **Elena V. Valeeva:** Formal analysis, Investigation, Writing – review & editing. **Agboigba Esperant Elvis Cokou:** Investigation, Writing – review & editing. **Shamil Z. Validov:** Investigation, Resources, Writing – review & editing. **Gyuzel A. Timerbulatova:** Investigation, Methodology, Writing – original draft, Writing – review & editing.

Declaration of Competing Interest

The authors declare no conflict of interest.

Data availability

Data will be made available on request.

Acknowledgments

The study was funded by the Russian Science Foundation grant N°22-25-00512, https://rscf.ru/en/project/22-25-00512/.

The authors thank the Interdisciplinary Center for Analytical Microscopy of Kazan Federal University for valuable support.

Appendix A. Supplementary data

Supplementary data to this article can be found online at https://doi.org/10.1016/j.taap.2023.116784.

References

Ajori, S., Ansari, R., Darvizeh, M., 2015. Vibration characteristics of single- and double-walled carbon nanotubes functionalized with amide and amine groups. Phys. B Condens. Matter 462, 8–14. https://doi.org/10.1016/j.physb.2015.01.003.

Alarifi, S., Ali, D., 2015. Mechanisms of Multi-walled Carbon Nanotubes–Induced Oxidative Stress and Genotoxicity in Mouse Fibroblast Cells. Int. J. Toxicol. 34 (3), 258–265. https://doi.org/10.1177/1091581815584799.

Azad, N., Iyer, A.K., Wang, L., Liu, Y., Lu, Y., Rojanasakul, Y., 2013. Reactive oxygen species-mediated p38 MAPK regulates carbon nanotube-induced fibrogenic and angiogenic responses. Nanotoxicology. 7 (2), 157–168. https://doi.org/10.3109/17435390.2011.647929.

Azqueta, A., Dusinska, M., 2015. The use of the comet assay for the evaluation of the genotoxicity of nanomaterials. Front. Genet. 6, 239. https://doi.org/10.3389/fgene.2015.00239.

Azqueta, A., Stopper, H., Zegura, B., Dusinska, M., Møller, P., 2022. Do cytotoxicity and cell death cause false positive results in the in vitro comet assay? Mutat. Res./Genet. Toxicol. Environ. Mutagenesis. 881, 503520 https://doi.org/10.1016/j.mrgentox.2022.503520.

Bargagli, E., Olivieri, C., Bennett, D., Prasse, A., Muller-Quernheim, J., Rottoli, P., 2009. Oxidative stress in the pathogenesis of diffuse lung diseases: a review. Respir. Med. 103 (9), 1245–1256. https://doi.org/10.1016/j.rmed.2009.04.014.

Chakravarthy, A., Khan, L., Bensler, N.P., Bose, P., De Carvalho, D.D., 2018. TGF-β-associated extracellular matrix genes link cancer-associated fibroblasts to immune evasion and immunotherapy failure. Nat. Commun. 9, 4692. https://doi.org/10.1038/s41467-018-06654-8.

Chen, R.J., Bangsaruntip, S., Drouvalakis, K.A., et al., 2003. Noncovalent functionalization of carbon nanotubes for highly specific electronic biosensors. Proc. Natl. Acad. Sci. U. S. A. 100 (9), 4984–4989. https://doi.org/10.1073/pnas.0837064100.

Chen, M., Zhao, G., Shao, L.L., et al., 2017. Controlled synthesis of nickel encapsulated into nitrogen-doped carbon nanotubes with covalent bonded interfaces: the structural and electronic modulation strategy for an efficient Electrocatalyst in dye-sensitized solar cells. Chem. Mater. 29, 9680–9694. https://doi.org/10.1021/acs.chemmater. 7b03385.s001.

Chen, M., Wang, G.C., Shao, L.L., et al., 2018. Strategic design of vacancy-enriched Fe1-xS nanoparticles anchored on Fe3C-encapsulated and N-doped carbon nanotube hybrids for high-efficiency triiodide reduction in dye-sensitized solar cells. ACS Appl. Mater. Interfaces 10 (37), 31208–31224. https://doi.org/10.1021/acsami.8b08489.

Chen, M., Jing, Q.S., Sun, H.B., et al., 2019a. Engineering the Core-Shell-structured NCNT-Ni2Si@porous Si composite with robust Ni-Si interfacial bonding for high-performance Li-ion batteries. Langmuir. 35 (19), 6321–6332. https://doi.org/10.1021/acs.langmuir.9b00558.

Chen, M., Wang, G.C., Yang, W.Q., et al., 2019b. Enhanced synergetic catalytic effect of Mo2C/NCNT@co Heterostructures in dye-sensitized solar cells: fine-tuned energy level alignment and efficient charge transfer behavior. ACS Appl. Mater. Interfaces 11 (45), 42156–42171. https://doi.org/10.1021/acsami.9b14316.

Chen, M., Shao, L.L., Lv, X.W., et al., 2020. In situ growth of Niencapsulated and N-doped carbon nanotubes on N-doped ordered mesoporous carbon for high-efficiency triiodide reduction in dye-sensitized solar cells. Chem. Eng. J. 390, 124633 https://doi.org/10.1016/j.cej.2020.124633.

Chernova, T., Murphy, F.A., Galavotti, S., Sun, X.M., Powley, I.R., Grosso, S., Schinwald, A., Zacarias-Cabeza, J., Dudek, K.M., Dinsdale, D., Le Quesne, J., Bennett, J., Nakas, A., Greaves, P., Poland, C.A., Donaldson, K., Bushell, M., Willis, A.E., MacFarlane, M., 2017. Long-Fiber carbon nanotubes replicate Asbestos-induced mesothelioma with disruption of the tumor suppressor gene Cdkn2a (Ink4a/Arf). Curr. Biol. 27 (21), 3302–3314.e6. https://doi.org/10.1016/j.cub.2017.09.007.

Cherukuri, P., Bachilo, S.M., Litovsky, S.H., Weisman, R.B., 2004. Near-infrared fluorescence microscopy of single-walled carbon nanotubes in phagocytic cells. J. Am. Chem. Soc. 126 (48), 15638–15639. https://doi.org/10.1021/ja0466311.

Di Giorgio, M.L., Di Bucchianico, S., Ragnelli, A.M., Aimola, P., Santucci, S., Poma, A., 2011. Effects of single and multiwalled carbon nanotubes on macrophages: cyto and genotoxicity and electron microscopy. Mutat. Res. 722 (1), 20–31. https://doi.org/10.1016/j.mrgentox.2011.02.008.

Di Ianni, E., Erdem, J.S., Møller, P., et al., 2021. In vitro-in vivo correlations of pulmonary inflammogenicity and genotoxicity of MWCNT. Part. Fibre Toxicol. 18 (1), 25. https://doi.org/10.1186/s12989-021-00413-2.

Dong, J., Ma, Q., 2019. Integration of inflammation, fibrosis, and cancer induced by carbon nanotubes. Nanotoxicology. 13 (9), 1244–1274. https://doi.org/10.1080/17435390.2019.1651920.

Dresselhaus, M.S., Dresselhaus, G., Saito, R., Jorio, A., 2005. Raman spectroscopy of carbon nanotubes. Phys. Rep. 409 (2), 47–99. https://doi.org/10.1016/j.physrep.2004.10.006.

Eatemadi, A., Daraee, H., Karimkhanloo, H., et al., 2014. Carbon nanotubes: properties, synthesis, purification, and medical applications. Nanoscale Res. Lett. 9 (1), 393. https://doi.org/10.1186/1556-276X-9-393.

Ema, M., Takehara, H., Naya, M., et al., 2017. Length effects of single-walled carbon nanotubes on pulmonary toxicity after intratracheal instillation in rats. Toxicol. Sci. 42 (3), 367–378. https://doi.org/10.2131/jts.42.367.

Erdely, A., Dahm, M., Chen, B.T., et al., 2013. Carbon nanotube dosimetry: from workplace exposure assessment to inhalation toxicology. Part. Fibre Toxicol. 10 (1), 53. https://doi.org/10.1186/1743-8977-10-53.

Esfandiary, E., Valiani, A., Hashemibeni, B., Moradi, I., Narimani, M., 2014. The evaluation of toxicity of carbon nanotubes on the human adipose-derived-stem cells in-vitro, 3, 40. https://doi.org/10.4103/2277-9175.125729.

Fatkhutdinova, L.M., Khaliullin, T.O., Vasil'yeva, O.L., et al., 2016. Fibrosis biomarkers in workers exposed to MWCNT. Toxicol. Appl. Pharmacol. 299, 125–131. https://doi.org/10.1016/j.taap.2016.02.016.

Fraser, K., Kodali, V., Yanamala, N., et al., 2020. Physicochemical characterization and genotoxicity of the broad class of carbon nanotubes and nanofibers used or produced in U.S. facilities. Part. Fibre Toxicol. 17, 62. https://doi.org/10.1186/s12989-020-00392-w.

Fujita, K., Obara, S., Maru, J., 2021. Pulmonary toxicity, cytotoxicity, and genotoxicity of submicron-diameter carbon fibers with different diameters and lengths. Toxicology. 466, 153063. https://doi.org/10.1016/j.tox.2021.153063.

Fukai, E., Sato, H., Watanabe, M., Nakae, D., Totsuka, Y., 2018. Establishment of an in vivo simulating co-culture assay platform for genotoxicity of multi-walled carbon nanotubes. Cancer Sci. 109 (4), 1024–1031. https://doi.org/10.1111/cas.13534.

Gabidinova, G.F., Timerbulatova, G.A., Daminova, A.G., Galyaltdinov, S.F., Dimiev, A. M., Kryuchkova, M.A., Fakhrullin, R.F., Fatkhutdinova, L.M., 2022. Evaluation of the impact of industrial single-walled and multi-walled carbon nanotubes on human respiratory tract epithelial cells. Hyg. Sanit. 101 (12), 1509–1520. https://doi.org/10.47470/0016-9900-2022-101-12-1509-1520. (in Russian).

García-Rodríguez, A., Rubio, L., Vila, L., Xamena, N., Velázquez, A., Marcos, R., Hernández, A., 2019. The comet assay as a tool to detect the genotoxic potential of nanomaterials. Nanomaterials. 9 (10), 1385. https://doi.org/10.3390/nano9101385.

Grosse, Y., Loomis, D., Guyton, K.Z., et al., 2014. Carcinogenicity of fluoro-edenite, silicon carbide fibres and whiskers, and carbon nanotubes. Lancet Oncol. 15 (13), 1427–1428. https://doi.org/10.1016/S1470-2045(14)71109-X.

Guo, F., Kang, T., Liu, Z., et al., 2019. Advanced Lithium metal-carbon nanotube composite anode for high-performance Lithium-oxygen batteries. Nano Lett. 19 (9), 6377–6384. https://doi.org/10.1021/acs.nanolett.9b02560.

Hassan, A.G., Mat Yajid, M.A., Saud, S.N., et al., 2020. Effects of varying electrodeposition voltages on surface morphology and corrosion behavior of multi-walled carbon nanotube coated on porous Ti-30 at. %-ta shape memory alloys. Surf. Coat. Technol. 401, 126257 https://doi.org/10.1016/j.surfcoat.2020.126257.

He, X., Young, S.H., Schwegler-Berry, D., Chisholm, W.P., Fernback, J.E., Ma, Q., 2011. Multiwalled carbon nanotubes induce a fibrogenic response by stimulating reactive oxygen species production, activating NF-κB signaling, and promoting fibroblast-to-myofibroblast transformation. Chem. Res. Toxicol. 24 (12), 2237–2248. https://doi.org/10.1021/tx200351d.

He, X., Young, S.H., Fernback, J.E., Ma, Q., 2012. Single-walled carbon nanotubes induce Fibrogenic effect by disturbing mitochondrial oxidative stress and activating NF-κB signaling. J. Clin. Toxicol. Supple 5, 5. https://doi.org/10.4172/2161-0495.S5-005.

Hojo, M., Maeno, A., Sakamoto, Y., Ohnuki, A., Tada, Y., Yamamoto, Y., Ikushima, K., Inaba, R., Suzuki, J., Taquahashi, Y., et al., 2022. Two-year intermittent exposure of a multiwalled carbon nanotube by intratracheal instillation induces lung tumors and pleural mesotheliomas in F344 rats. Part. Fibre Toxicol. 19, 38. https://doi.org/10.1186/s12989-022-00478-7.

Honda, K., Naya, M., Takehara, H., Kataura, H., Fujita, K., Ema, M., 2017. A 104-week pulmonary toxicity assessment of long and short single-wall carbon nanotubes after a single intratracheal instillation in rats. Inhal. Toxicol. 29 (11), 471–482. https://doi.org/10.1080/08958378.2017.1394930.

Inghilleri, S., Morbini, P., Oggionni, T., Barni, S., Fenoglio, C., 2006. In situ assessment of oxidant and nitrogenic stress in bleomycin pulmonary fibrosis. Histochem. Cell Biol. 125 (6), 661–669. https://doi.org/10.1007/s00418-005-0116-7.

ISO 10993-5:2009, 2009. Biological Evaluation of Medical Devices - Part 5: Tests for in Vitro Cytotoxicity. International Organization for Standardization.

Janudin, N., Abdullah, N., Wan Yunus, W.M.Z., et al., 2018. Effect of functionalized carbon nanotubes in the detection of benzene at room temperature. J. Nanotechnol. 2018, 2107898. https://doi.org/10.1155/2018/2107898.

Kalluri, R., Weinberg, R.A., 2009. The basics of epithelial-mesenchymal transition. J. Clin. Invest. 119, 1420–1428. https://doi.org/10.1172/JCI39104.

Khaliullin, T.O., Zalyalov, R.R., Fatkhutdinova, L.M., Shvedova, A.A., Kisin, E.R., 2015b. Evaluation of fibrogenic potential of industrial multi-walled carbon nanotubes in acute aspiration experiment. Bull. Exp. Biol. Med. 158, 684–687.

Kim, J.S., Yu, I.J., 2014. Single-Wall carbon nanotubes (SWCNT) induce cytotoxicity and genotoxicity produced by reactive oxygen species (ROS) generation in Phytohemagglutinin (PHA)-stimulated male human peripheral blood lymphocytes. J. Toxicol. Environ. Health A 77 (19), 1141–1153. https://doi.org/10.1080/15287394.2014.917062.

Kim, J.S., Song, K.S., Yu, I.J., 2015. Multiwall carbon nanotube-induced DNA damage and cytotoxicity in male human peripheral blood lymphocytes. Int. J. Toxicol. 35 (1), 27–37. https://doi.org/10.1177/1091581815598749.

Knudsen, K.B., Berthing, T., Jackson, P., et al., 2019. Physicochemical predictors of multi-walled carbon nanotube-induced pulmonary histopathology and toxicity one year after pulmonary deposition of 11 different multi-walled carbon nanotubes in mice. Basic Clin. Pharmacol. Toxicol. 124 (2), 211–227. https://doi.org/10.1111/bcpt.13119.

Kohl, Y., Rundén-Pran, E., Mariussen, E., et al., 2020. Genotoxicity of nanomaterials: advanced in vitro models and high throughput methods for human Hazard assessment-a review. Nanomaterials (Basel). 10 (10), 1911. https://doi.org/10.3390/nano10101911.

Lan, J., Gou, N., Gao, C., He, M., Gu, A.Z., 2014. Comparative and mechanistic genotoxicity assessment of nanomaterials via a quantitative toxicogenomics approach across multiple species. Environ. Sci. Technol. 48 (21), 12937–12945. https://doi.org/10.1021/es503065q.

Lindberg, H.K., Falck, G.C., Singh, R., et al., 2013. Genotoxicity of short single-wall and multi-wall carbon nanotubes in human bronchial epithelial and mesothelial cells in vitro. Toxicology. 313 (1), 24–37. https://doi.org/10.1016/j.tox.2012.12.008.

Liu, Z., Tabakman, S., Welsher, K., Dai, H., 2009. Carbon nanotubes in biology and medicine: in vitro and in vivo detection, imaging and drug delivery. Nano Res. 2 (2), 85–120. https://doi.org/10.1007/s12274-009-9009-8.

Livak, K.J., Schmittgen, T.D., 2001. Analysis of relative gene expression data using real-time quantitative PCR and the 2(-Delta Delta C(T)) method. Methods. 25, 402–408. https://doi.org/10.1006/meth.2001.1262.

Louro, H., Pinhão, M., Santos, J., Tavares, A., Vital, N., Silva, M.J., 2016. Evaluation of the cytotoxic and genotoxic effects of benchmark multi-walled carbon nanotubes in relation to their physicochemical properties. Toxicol. Lett. 262, 123–134. https://doi.org/10.1016/j.toxlet.2016.09.016.

Ma, Q., 2010. Transcriptional responses to oxidative stress: pathological and toxicological implications. Pharmacol. Ther. 125 (3), 376–393. https://doi.org/10.1016/j.pharmthera.2009.11.004.

Maity, D., Rajavel, K., Kumar, R.T.R., 2018. Polyvinyl alcohol wrapped multiwall carbon nanotube (MWCNT) network on fabrics for wearable room temperature ethanol sensor. Sensors Actuators B Chem. 261, 297–306. https://doi.org/10.1016/j.snb.2018.01.152.

Manke, A., Luanpitpong, S., Dong, C., Wang, L., He, X., Battelli, L., Derk, R., Stueckle, T. A., Porter, D.W., Sager, T., Gou, H., Dinu, C.Z., Wu, N., Mercer, R.R., Rojanasakul, Y., 2014. Effect of fiber length on carbon nanotube-induced fibrogenesis. Int. J. Mol. Sci. 15 (5), 7444–7461. https://doi.org/10.3390/ijms15057444.

Manshian, B.B., Jenkins, G.J.S., Williams, P.M., Wright, C., Barron, A.R., Brown, A.P., Hondow, N., Dunstan, P.R., Rickman, R., Brady, K., Doak, S.H., 2013. Single-walled carbon nanotubes: differential genotoxic potential associated with physico-chemical properties. Nanotoxicology. 7 (2), 144–156. https://doi.org/10.3109/17435390.2011.647928.

May, S., Hirsch, C., Rippl, A., Bürkle, A., Wick, P., 2022. Assessing genotoxicity of ten different engineered nanomaterials by the novel semi-automated FADU assay and the alkaline comet assay. Nanomaterials (Basel). 12 (2), 220. https://doi.org/10.3390/nano12020220.

Mercer, R.R., Scabilloni, J.F., Hubbs, A.F., Battelli, L.A., McKinney, W., Friend, S., Wolfarth, M.G., Andrew, M., Castranova, V., Porter, D.W., 2013. Distribution and fibrotic response following inhalation exposure to multi-walled carbon nanotubes. Part. Fibre Toxicol. 10, 33. https://doi.org/10.1186/1743-8977-10-33.

Migliore, L., Saracino, D., Bonelli, A., et al., 2010. Carbon nanotubes induce oxidative DNA damage in RAW 264.7 cells. Environ. Mol. Mutagen. 51 (4), 294–303. https://doi.org/10.1002/em.20545.

Mishra, A., Rojanasakul, Y., Chen, B.T., Castranova, V., Mercer, R.R., Wang, L., 2012. Assessment of pulmonary Fibrogenic potential of multiwalled carbon nanotubes in human lung cells. J. Nanomater. 13 (1), 27. https://doi.org/10.1155/2012/930931.

Mishra, A., Stueckle, T.A., Mercer, R.R., et al., 2015. Identification of TGF-β receptor-1 as a key regulator of carbon nanotube-induced fibrogenesis. Am. J. Phys. Lung Cell. Mol. Phys. 309 (8), L821–L833. https://doi.org/10.1152/ajplung.00002.2015.

Møller, P., Christophersen, D.V., Jensen, D.M., et al., 2014. Role of oxidative stress in carbon nanotube-generated health effects. Arch. Toxicol. 88 (11), 1939–1964. https://doi.org/10.1007/s00204-014-1356-x.

Møller, P., Wils, R.S., Di Ianni, E., Gutierrez, C.A.T., Roursgaard, M., Jacobsen, N.R., 2021. Genotoxicity of multi-walled carbon nanotube reference materials in mammalian cells and animals. Mutat. Res. Rev. Mutat. Res. 788, 108393 https://doi.org/10.1016/j.mrrev.2021.108393.

Murray, A.R., Kisin, E., Leonard, S.S., Young, S.H., Kommineni, C., Kagan, V.E., Shvedova, A.A., 2009. Oxidative stress and inflammatory response in dermal toxicity of single-walled carbon nanotubes. Toxicology. 257 (3), 161–171. https://doi.org/10.1016/j.tox.2008.12.023.

Mutlu, M.G., Budinger, G.R.S., Green, A.A., et al., 2010. Biocompatible nanoscale dispersion of single-walled carbon nanotubes minimizes in vivo pulmonary toxicity. Nano Lett. 10 (5), 1664–1670. https://doi.org/10.1021/nl9042483.

Nagai, H., Okazaki, Y., Chew, S.H., Misawa, N., Miyata, Y., Shinohara, H., Toyokuni, S., 2013. Intraperitoneal administration of tangled multiwalled carbon nanotubes of 15nm in diameter does not induce mesothelial carcinogenesis in rats. Pathol. Int. 63 (9), 457–462. https://doi.org/10.1111/pin.12093.

NIOSH—National Institute of Occupational safety and Health. Current Intelligence Bulletin 65—Occupational Exposure to Carbon Nanotubes and Nanofibers. Centers for Disease Control and Prevention, National Institute for Occupational Safety and Health; Cincinnati, OH, USA: 2013. pp. 2013–2145. Department of Health and Human Services.

Nurazzi, N.M., Asyraf, M.R.M., Khalina, A., et al., 2021a. Fabrication, functionalization, and application of carbon nanotube-reinforced polymer composite: an overview. Polymers (Basel). 13 (7), 1047. https://doi.org/10.3390/polym13071047.

Nurazzi, N.M., Harussani, M.M., Siti Zulaikha, N.D., et al., 2021b. Composites based on conductive polymer with carbon nanotubes in DMMP gas sensors – an overview. Polimery. 66, 85–97. https://doi.org/10.3390/polym13071047.

Öner, D., Ghosh, M., Bové, H., et al., 2018. Differences in MWCNT- and SWCNT-induced DNA methylation alterations in association with the nuclear deposition. Part. Fibre Toxicol. 15 (1), 11. https://doi.org/10.1186/s12989-018-0244-6.

Pardali, E., Sanchez-Duffhues, G., Gomez-Puerto, M.C., Ten Dijke, P., 2017. TGF-β-induced endothelial-mesenchymal transition in fibrotic diseases. Int. J. Mol. Sci. 18 (10), 2157. https://doi.org/10.3390/ijms18102157.

Poland, C., Duffin, R., Kinloch, I., et al., 2008. Carbon nanotubes introduced into the abdominal cavity of mice show asbestos-like pathogenicity in a pilot study. Nat. Nanotech. 3, 423–428. https://doi.org/10.1038/nnano.2008.111.

Polimeni, M., Gulino, G.R., Gazzano, E., et al., 2016. Multi-walled carbon nanotubes directly induce epithelial-mesenchymal transition in human bronchial epithelial cells via the TGF-β-mediated Akt/GSK-3β/SNAIL-1 signalling pathway. Part. Fibre Toxicol. 13 (1), 27. https://doi.org/10.1186/s12989-016-0138-4.

Pothmann, D., Simar, S., Schuler, D., et al., 2015. Lung inflammation and lack of genotoxicity in the comet and micronucleus assays of industrial multiwalled carbon nanotubes Graphistrength(©) C100 after a 90-day nose-only inhalation exposure of rats. Part. Fibre Toxicol. 12, 21. https://doi.org/10.1186/s12989-015-0096-2.

Poulsen, S.S., Jackson, P., Kling, K., et al., 2016. Multi-walled carbon nanotube physicochemical properties predict pulmonary inflammation and genotoxicity. Nanotoxicology. 10 (9), 1263–1275. https://doi.org/10.1080/17435390.2016.1202351.

Predtechenskiy, M.R., Khasin, A.A., Bezrodny, A.E., Bobrenok, O.F., Dubov, D.Yu., Muradyan, V.E., Saik, V.O., Smirnov, S.N., 2022a. New perspectives in SWCNT

applications: Tuball SWCNT. Part 1. Tuball by itself—all you need to know about it. Carbon Trends. 8, 100175 https://doi.org/10.1016/j.cartre.2022.100175.
Predtechenskiy, M.R., Khasin, A.A., Smirnov, S.N., Bezrodny, A.E., Bobrenok, O.F., Dubov, D.Yu., Kosolapov, A.G., Lyamysheva, E.G., Muradyan, V.E., Saik, V.O., Shinkarev, V.V., Chebochakov, D.S., Galkov, M.S., Karpunin, R.V., Verkhovod, T.D., Yudaev, D.V., Myasnikova, Yu.S., Krasulina, A.N., Lazarev, M.K., 2022b. New perspectives in SWCNT applications: Tuball SWCNT. Part 2. New Composite Materials through Augmentation with Tuball. Carbon Trends. 8, 100176 https://doi.org/10.1016/j.cartre.2022.100176.
Rahman, L., Jacobsen, N.R., Aziz, S.A., et al., 2017. Multi-walled carbon nanotube-induced genotoxic, inflammatory and pro-fibrotic responses in mice: investigating the mechanisms of pulmonary carcinogenesis. Mutat. Res. Genet. Toxicol. Environ. Mutagen. 823, 28–44. https://doi.org/10.1016/j.mrgentox.2017.08.005.
Sager, T., Porter, D., Robinson, V., Lindsley, W., Schwegler-Berry, D., Castranova, V., 2009. Improved method to disperse nanoparticles for in vitro and in vivo investigation of toxicity. Nanotoxicology. 1, 118–129. https://doi.org/10.1080/17435390701381596.
Sakamoto, Y., Nakae, D., Fukumori, N., Tayama, K., Maekawa, A., Imai, K., Hirose, A., Nishimura, Y., Ohashi, N., Ogata, A., 2009. Induction of mesothelioma by a single intrascrotal administration of multi-wall carbon nanotube in intact male Fischer 344 rats. J. Toxicol. Sci. 34, 65–76. https://doi.org/10.2131/jts.34.65.
Samadian, H., Salami, M.S., Jaymand, M., Azarnezhad, A., Najafi, M., Barabadi, H., Ahmadi, A., 2020. Genotoxicity assessment of carbon-based nanomaterials; have their unique physicochemical properties made them double-edged swords? Mutat. Res./Rev. Mutat. Res. 108296 https://doi.org/10.1016/j.mrrev.2020.108296.
Sargent, L.M., Hubbs, A.F., Young, S.H., et al., 2012. Single-walled carbon nanotube-induced mitotic disruption. Mutat. Res. 745 (1–2), 28–37. https://doi.org/10.1016/j.mrgentox.2011.11.017.
Sargent, L.M., Porter, D.W., Staska, L.M., et al., 2014. Promotion of lung adenocarcinoma following inhalation exposure to multi-walled carbon nanotubes. Part. Fibre Toxicol. 11, 3. https://doi.org/10.1186/1743-8977-11-3.
Septiadi, D., Rodriguez-Lorenzo, L., Balog, S., et al., 2019. Quantification of carbon nanotube doses in adherent cell culture assays using UV-VIS-NIR spectroscopy. Nanomaterials (Basel). 9 (12), 1765. https://doi.org/10.3390/nano9121765.
Shvedova, A., Castranova, V., Kisin, E., Schwegler-Berry, D., Murray, A., Gandelsman, V., Baron, P., 2003. Exposure to carbon nanotube material: assessment of nanotube cytotoxicity using human keratinocyte cells. J. Toxicol. Environ. Health A 66 (20), 1909–1926. https://doi.org/10.1080/713853956.
Shvedova, A.A., Kisin, E.R., Mercer, R., et al., 2005. Unusual inflammatory and fibrogenic pulmonary responses to single-walled carbon nanotubes in mice. Am. J. Phys. Lung Cell. Mol. Phys. 289 (5), 698–708. https://doi.org/10.1152/ajplung.00084.2005.
Shvedova, A.A., Kisin, E.R., Murray, A.R., et al., 2007. Vitamin E deficiency enhances pulmonary inflammatory response and oxidative stress induced by single-walled carbon nanotubes in C57BL/6 mice. Toxicol. Appl. Pharmacol. 221 (3), 339–348. https://doi.org/10.1016/j.taap.2007.03.018.
Shvedova, A.A., Kisin, E.R., Murray, A.R., et al., 2008. Inhalation vs. aspiration of single-walled carbon nanotubes in C57BL/6 mice: inflammation, fibrosis, oxidative stress, and mutagenesis. Am. J. Phys. Lung Cell. Mol. Phys. 295 (4), 552–565. https://doi.org/10.1152/ajplung.90287.2008.
Shvedova, A.A., Pietroiusti, A., Fadeel, B., Kagan, V.E., 2012. Mechanisms of carbon nanotube-induced toxicity: focus on oxidative stress. Toxicol. Appl. Pharmacol. 261 (2), 121–133. https://doi.org/10.1016/j.taap.2012.03.023.
Shvedova, A.A., Yanamala, N., Kisin, E.R., et al., 2014. Long-term effects of carbon containing nanomaterials and asbestos in the lung: one year postexposure comparisons. Am. J. Phys. Lung Cell. Mol. Phys. 306 (2), 170–182. https://doi.org/10.1152/ajplung.00167.2013.
Shvedova, A.A., Yanamala, N., Kisin, E.R., Khailullin, T.O., Birch, M.E., Fatkhutdinova, L.M., 2016. Integrated analysis of dysregulated ncRNA and mRNA expression profiles in humans exposed to carbon nanotubes. PLoS One 11 (3), e0150628. https://doi.org/10.1371/journal.pone.0150628.
Shvedova, A.A., Tkach, A.V., Kisin, E.R., et al., 2013. Carbon nanotubes enhance metastatic growth of lung carcinoma via up-regulation of myeloid-derived suppressor cells. Small. 9 (9–10), 1691–1695. https://doi.org/10.1002/smll.201201470.
Siegrist, K.J., Reynolds, S.H., Kashon, M.L., et al., 2014. Genotoxicity of multi-walled carbon nanotubes at occupationally relevant doses. Part. Fibre Toxicol. 11, 6. https://doi.org/10.1186/1743-8977-11-6.
Siegrist, K.J., Reynolds, S.H., Porter, D.W., et al., 2019. Mitsui-7, heat-treated, and nitrogen-doped multi-walled carbon nanotubes elicit genotoxicity in human lung epithelial cells. Part. Fibre Toxicol. 16 (1), 36. https://doi.org/10.1186/s12989-019-0318-0.
Snyder-Talkington, B.N., Dong, C., Sargent, L.M., et al., 2016. mRNAs and miRNAs in whole blood associated with lung hyperplasia, fibrosis, and bronchiolo-alveolar adenoma and adenocarcinoma after multi-walled carbon nanotube inhalation exposure in mice. J. Appl. Toxicol. 36 (1), 161–174. https://doi.org/10.1002/jat.3157.
Solorio-Rodriguez, S.A., Williams, A., Poulsen, S.S., et al., 2023. Single-walled vs. multi-walled carbon nanotubes: influence of Physico-chemical properties on Toxicogenomics responses in mouse lungs. Nanomaterials (Basel). 13 (6), 1059. https://doi.org/10.3390/nano13061059.
Souto, L.F.C., Soares, B.G., 2020. Polyaniline/carbon nanotube hybrids modified with ionic liquids as anticorrosive additive in epoxy coatings. Prog. Org. Coat. 143, 105598 https://doi.org/10.1016/j.porgcoat.2020.105598.
Suzui, M., Futakuchi, M., Fukamachi, K., et al., 2016. Multiwalled carbon nanotubes intratracheally instilled into the rat lung induce development of pleural malignant mesothelioma and lung tumors. Cancer Sci. 107 (7), 924–935. https://doi.org/10.1111/cas.12954.
Takagi, A., Hirose, A., Nishimura, T., Fukumori, N., Ogata, A., Ohashi, A., Kitajima, S., Kanno, J., 2008. Induction of mesothelioma in p53+/− mouse by intraperitoneal application of multi-wall carbon nanotube. J. Toxicol. Sci. 33, 105–116. https://doi.org/10.2131/jts.33.105.
Takagi, A., Hirose, A., Futakuchi, M., Tsuda, H., Kanno, J., 2012. Dose-dependent mesothelioma induction by intraperitoneal administration of multi-wall carbon nanotubes in p53 heterozygous mice. Cancer Sci. 103, 1440–1444. https://doi.org/10.1111/j.1349-7006.2012.02318.x.
Teeguarden, J.G., Webb-Robertson, B.J., Waters, K.M., et al., 2011. Comparative proteomics and pulmonary toxicity of instilled single-walled carbon nanotubes, crocidolite asbestos, and ultrafine carbon black in mice. Toxicol. Sci. 120 (1), 123–135. https://doi.org/10.1093/toxsci/kfq363.
Timerbulatova, G.A., Dimiev, A.M., Khamidullin, T.L., et al., 2020. Dispersion of single-walled carbon nanotubes in biocompatible media. Russian Nanotechnol. 15 (4), 461–469. https://doi.org/10.1134/S1992722320040160. (in Russian).
Timerbulatova, G.A., Dunaev, P.D., Dimiev, A.M., Gabidinova, G.F., Khaertdinov, N.N., Fakhrullin, R.F., Boichuk, S.V., Fatkhutdinova, L.M., 2021. Comparative characteristics of various fibrous materials in in vitro experiments. Kazan Med. J. 102 (4), 501–509. https://doi.org/10.17816/KMJ2021-501. (in Russian).
Tkachev, A.G., Melezhik, A.V., Dyachkova, T.P., Blokhin, A.N., Burakova, E.A., Pas'ko, T.V., 2013. Carbon nanomaterials of the Taunit series: production and application. News of higher educational institutions. Chemi. Chem. Technol. 56 (4), 55–59 (in Russian).
Ursini, C.L., Cavallo, D., Fresegna, A.M., et al., 2014. Differences in cytotoxic, genotoxic, and inflammatory response of bronchial and alveolar human lung epithelial cells to pristine and COOH-functionalized multiwalled carbon nanotubes. Biomed. Res. Int. 2014, 359506 https://doi.org/10.1155/2014/359506.
Vales, G., Rubio, L., Marcos, R., 2016. Genotoxic and cell-transformation effects of multi-walled carbon nanotubes (MWCNT) following in vitro sub-chronic exposures. J. Hazard. Mater. 306, 193–202. https://doi.org/10.1016/j.jhazmat.2015.12.021.
van Berlo, D., Clift, M.J., Albrecht, C., Schins, R.P., 2012. Carbon nanotubes: an insight into the mechanisms of their potential genotoxicity. Swiss Med. Wkly. 142, w13698 https://doi.org/10.4414/smw.2012.13698.
Ventura, C., Pereira, J.F.S., Matos, P., et al., 2020. Cytotoxicity and genotoxicity of MWCNT-7 and crocidolite: assessment in alveolar epithelial cells versus their coculture with monocyte-derived macrophages [published correction appears in Nanotoxicology. 2022 May;16(4):547]. Nanotoxicology 14 (4), 479–503. https://doi.org/10.1080/17435390.2019.1695975.
Vietti, G., Lison, D., van den Brule, S., 2016. Mechanisms of lung fibrosis induced by carbon nanotubes: towards an adverse outcome pathway (AOP). Part. Fibre Toxicol. 13, 11. https://doi.org/10.1186/s12989-016-0123-y.
Wang, L., Castranova, V., Mishra, A., et al., 2010. Dispersion of single-walled carbon nanotubes by a natural lung surfactant for pulmonary in vitro and in vivo toxicity studies. Part. Fibre Toxicol. 7, 31. https://doi.org/10.1186/1743-8977-7-31.
Wang, X., Xia, T., Ntim, S.A., Ji, Z., Lin, S., Meng, H., Chung, C.H., George, S., Zhang, H., Wang, M., et al., 2011. Dispersal state of multiwalled carbon nanotubes elicits profibrogenic cellular responses that correlate with fibrogenesis biomarkers and fibrosis in the murine lung. ACS Nano 5, 9772–9787. https://doi.org/10.1021/nn2033055.
Wang, X., Duch, M.C., Mansukhani, N., Ji, Z., Liao, Y.P., Wang, M., Zhang, H., Sun, B., Chang, C.H., Li, R., et al., 2015. Use of a pro-fibrogenic mechanism-based predictive toxicological approach for tiered testing and decision analysis of carbonaceous nanomaterials. ACS Nano 9, 3032–3043. https://doi.org/10.1021/nn507243w.
Wang, X., Mansukhani, N.D., Guiney, L.M., et al., 2016. Toxicological profiling of highly purified metallic and semiconducting single-walled carbon nanotubes in the rodent lung and E. Coli. ACS Nano 10 (6), 6008–6019. https://doi.org/10.1021/acsnano.6b01560.
Wils, R.S., Jacobsen, N.R., Di Ianni, E., Roursgaard, M., Møller, P., 2021a. Reactive oxygen species production, genotoxicity and telomere length in FE1-Muta™mouse lung epithelial cells exposed to carbon nanotubes. Nanotoxicology. 15 (5), 661–672. https://doi.org/10.1080/17435390.2021.1910359.
Wils, R.S., Jacobsen, N.R., Vogel, U., Roursgaard, M., Møller, P., 2021b. Inflammatory response, reactive oxygen species production and DNA damage in mice after Intrapleural exposure to carbon nanotubes. Toxicol. Sci. 183 (1), 184–194. https://doi.org/10.1093/toxsci/kfab070.
Zhou, E., Xi, J., Guo, Y., et al., 2018. Synergistic effect of graphene and carbon nanotube for high-performance electromagnetic interference shielding films. Carbon. 133, 316–322. https://doi.org/10.1016/j.carbon.2018.03.023.

Web references

State Pharmacopoeia of the Russian Federation, 2018. XIV ed., Approved by order of the Ministry of Health of the Russian Federation dated October 31. https://femb.ru/record/pharmacopea14 (accessed 20 November 2023).